SEDIMENTOLOGY the journal of the International Association of Sedimentologists

Sedimentology (2011) **58,** 890–915 doi: 10.1111/j.1365-3091.2010.01188.x

Turbiditic, clay-rich event beds in fjord-marine deposits caused by landslides in emerging clay deposits – palaeoenvironmental interpretation and role for submarine mass-wasting

LOUISE HANSEN*, JEAN SEBASTIEN L'HEUREUX† and ODDVAR LONGVA*

**Geological Survey of Norway (NGU), Leiv Eirikssons vei 39, N-7491 Trondheim, Norway (E-mail: louise.hansen@ngu.no)*

†Norwegian University of Science and Technology (NTNU), Department of Civil and Transport Engineering, Geotechnical Division, Høgskoleringen 7A, N-7491 Trondheim, Norway

Associate Editor – Jess Trofimovs

ABSTRACT

Distinct, clay-rich beds are common in fjord-marine deposits in Trondheimsfjorden near the outlet of the Nidelva River. Their characteristic light-grey colour makes the beds easily distinguishable from the surrounding brownish, bioturbated, muddy fjord sediments. The clay-rich beds commonly display a clear stratification in clay, silt and very fine sand. The beds are interpreted as originating primarily from large quick-clay landslides upstream along the Nidelva River. Such events resulted in a sudden increase in the supply of fines to the fjord from disintegrating landslide debris and heavily loaded effluent plumes, possibly favouring hyperpycnal flow. Typical beds can be divided into a clay-rich lower section, reflecting an initial surge with high concentrations of suspended mud, and a sandier upper section reflecting pulses of higher energy. This development can be explained, for example, by a lowering in the supply of mud, an increasing activity of deltaic sediment gravity flows due to a higher availability of sandy sediments in the landslide-affected river, and by flooding and/or breaching of landslide dams. The typical, stratified beds are interpreted as the result of one quick-clay landslide, whereas exceptionally thick, less organized, stratified beds are possibly the result of several large and/or complex landslides. Radiocarbon dating of mollusc shells has helped to establish a chronology for major terrestrial landslides in the area. The frequency of landslides increases towards the end of the Holocene. This is explained by a progressively deeper incision of rivers during glacioisostatic rebound, possibly combined with a change to a wetter climate. The marine core record displays deformation structures and hiati representing submarine mass-wasting events, and supports the evidence that the clay-rich beds are weak layers in the fjord-marine stratigraphy. The inherent weakness of these layers may be explained by their composition, immature texture, loose fabric and contrasting permeabilities in the deposits. Slide-prone layers similar to the clay-rich beds described here may be found in other comparable fjord-marginal settings and are considered to be of importance for geohazard assessments.

Keywords Event bed, fjord, landslide, Norway, quick clay, turbidite.

INTRODUCTION

Event beds usually are deposited quickly as the result of exceptional happenings in a basin, such as a fjord or its catchment. These beds, sometimes also referred to as rapidly deposited layers, provide evidence of a range of processes and are commonly represented by turbidites, hyperpycnites or debris-flow deposits in marine or lacustrine records (e.g. Einsele *et al.*, 1996; Mulder *et al.*, 2001; Bøe *et al.*, 2003; St-Onge *et al.*, 2004; Schnellmann *et al.*, 2006). Usually, they are records of past landslides, earthquakes, floods or storms. Sedimentological and stratigraphic investigations of such beds may give important information on their origin, distribution, magnitudes, frequencies and depositional processes.

This study focuses on clay-rich event beds in the bay of Trondheim at the mouth of the river Nidelva in central Norway. The catchment of the river Nidelva has been affected by numerous quick-clay landslides during the Holocene with deposition of clay-rich beds in the fjord (L'Heureux *et al.*, 2009). The purpose of the present study is to analyse the sedimentology of the clay-rich beds, to interpret their depositional processes at various scales including a characterization of texture, fabric and microstructures, and to look for sedimentological characteristics that potentially play a role in submarine slope stability. Furthermore, the interplay between terrestrial landslides, river flow and fjord-marine processes, and the role of such beds in the overall fjord-marine stratigraphy, is outlined. A chronology for major terrestrial landslides is established based on radiocarbon dating.

SETTING

The bay of Trondheim is located in Trondheimsfjorden (Fig. 1). Depths increase northwards towards the central fjord basin which is *ca* 450 m deep (Fig. 1D). A bedrock high divides the embayment into a western part with a well-defined, deep, submarine channel system and an eastern part which is shallower. Detailed bathymetric data reveal a few pockmarks and numerous, sediment-draped, slide scars with planar centres (Fig. 1D). The stratigraphic succession displays an almost 100 m thick package of glaciomarine deposits overlain by fjord-marine sediments with several clay-rich beds (L'Heureux *et al.*, 2009). Bedrock in the catchment around Trondheim is dominated by chlorite-rich, Ordovician greenstone and greenschist of volcanic origin (Solli *et al.*, 2003). Onshore areas are dominated by fjord-marine and glaciomarine clays that emerged during the Holocene glacio-isostatic rebound of the area with a marine limit of *ca* 175 m above sea-level (a.s.l.). The fall of relative sea-level led to a northward progression of the river outlet. In the last 2000 to 3000 years, the outlet of the Nidelva River has shifted from the western part of the bay towards the east (Reite *et al.*, 1999; L'Heureux *et al.*, 2009; Fig. 1C).

The emerged clays are rich in illite, chlorite and a rock flour composed of quartz and feldspars (Selmer-Olsen, 1977). Subsequent long-term leaching of salts within the clays resulted in the formation of quick clay, which may liquefy during failure (Rosenquist, 1953), and large landslide scars in the area around Trondheim testify to major Holocene quick-clay failures (Reite, 1983; Sveian *et al.*, 2007; L'Heureux *et al.*, 2009). Dating of these landslide events is not straightforward as any organic matter suitable for dating may have been through several cycles of reworking (e.g. Hansen *et al.*, 2007). However, a first attempt to date quick-clay landslides in the Trondheim area from onshore investigations and historical records was presented by Sand (1999). Later, L'Heureux *et al.* (2009) provided a general chronological framework for the first recorded clay-rich beds in cores from the Trondheim bay.

DATA AND METHODS

High-resolution, swath bathymetric data from the Trondheim bay were acquired through several surveys between 2003 and 2009 using a 125 and 250 kHz GeoSwath interferometric sidescan sonar system (GeoAcoustics Limited, Great Yarmouth, UK). The resolution of the bathymetric data is within 1 m. Numerous seismic lines have been collected and one profile acquired by a high-frequency, parametric sonar Topas system is presented here. Thirty gravity cores, 47 short Niemestoe cores and one piston core (15 m) have been collected between 2005 and 2008. Core sites are shown in Fig. 1D and information on the cores presented here is summarized in Table 1. The cores were X-rayed and described visually to identify colour, lithology, sedimentary structures and fossils as a basis for facies analysis. Grain-size analyses were performed by laser diffraction using a Coulter LS 200 instrument (Coulter Corporation, Miami, FL, USA) and by hydrometer testing. Both methods have been applied on samples from the same level in one core (12) for comparison, and for outlining the variations by using the two methods. Sieve analysis was applied for some coarser samples.

Cores were analysed at intervals of 5 to 10 mm with regard to gamma density and magnetic susceptibility using a GEOTEK Multi Sensor Core

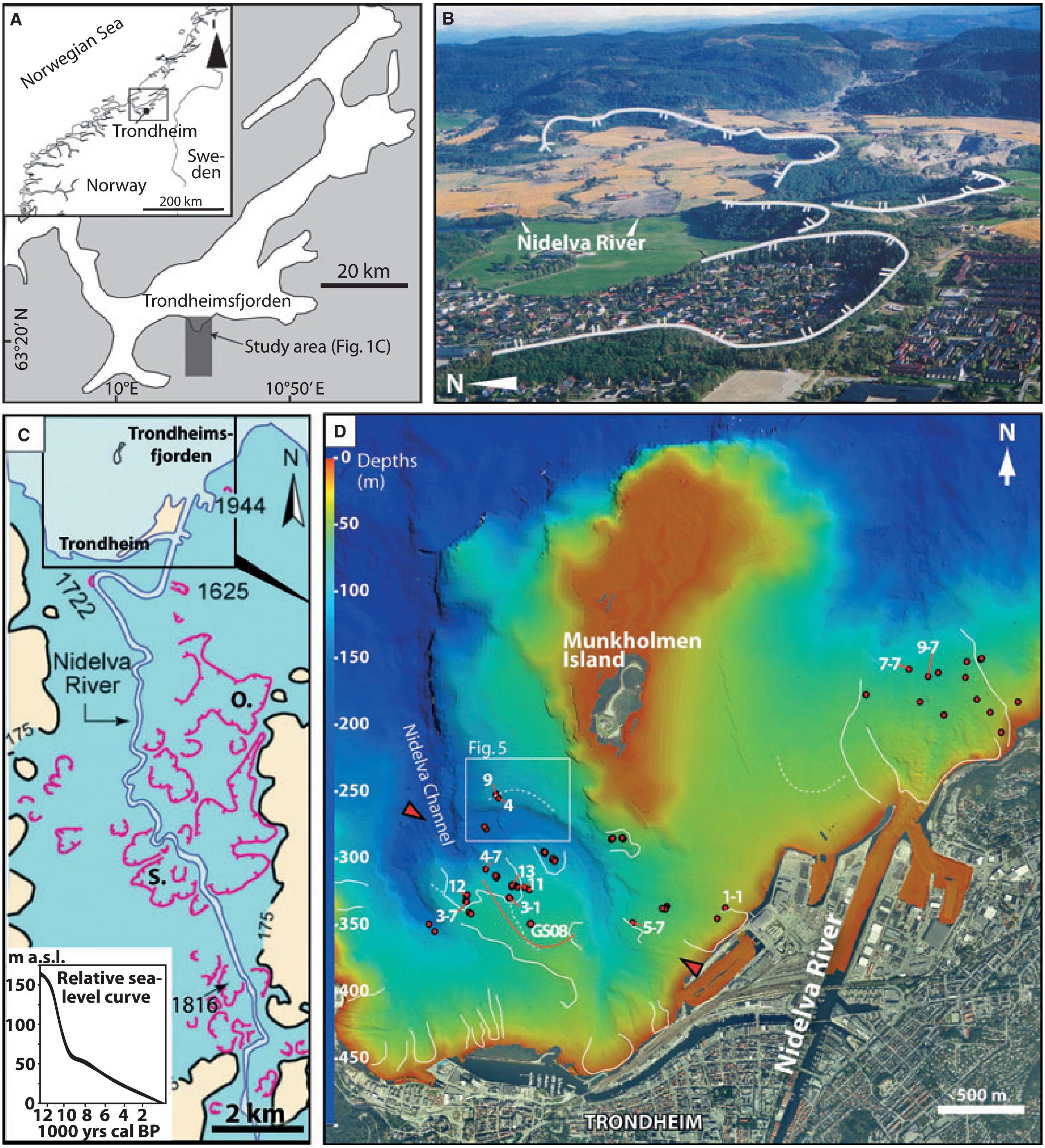

Fig. 1. (A) Location of the study area. (B) Slide scars (white lines) from prehistoric quick-clay landslides near Trondheim. (C) Scars (marked in red) after landslides in glacioisostatically elevated clay deposits along the Nidelva River and tributary rivers and relative sea-level curve (after Sveian *et al.*, 2007; L'Heureux *et al.*, 2009). The blue area represents thick (glacio)marine clays below a marine limit of 175 m a.s.l. This level represents the highest relative sea-level following the Ice Age, after which it fell to the present-day level. 'O': Othilienborg landslide; 'S': Sjetnemarka landslide. Newer slide scars are shown with the year, including the 1816 Tiller landslide. (D) Map of the Trondheim embayment with bathymetry. Core numbers are marked. A few selected submarine landslide scars are indicated by white lines, see also Hansen *et al.* (2005) and L'Heureux *et al.* (2009). Full lines indicate distinct, relatively young, slide scars while stippled lines indicate older, more diffuse, sediment-draped slide scars. Core information is given in Table 1. Red arrows indicate the approximate position of the schematic transect outlined in Fig. 4. The red line shows the position of the seismic section shown in Fig. 4.

Table 1. Information on cores used in this study.

Full name	Abbreviated name	Core type	Core length (cm)	Water depth (m)	N coordinate UTM sone 32 (WGS84)	E coordinate UTM sone 32 (WGS84)
0601004	4	Gravity	135	110	7036164	568341
0601009	9	Gravity	160	105	7036182	568327
0601011	11	Gravity	240	93?	7035645	568453
0601012	12	Gravity	210	91	7035596	568159
0601013	13	Gravity	175	90	7035657	568432
0701001	1-1	Gravity	160	28	7035521	569668
0701003	3-1	Gravity	375	81	7035582	568405
0707003	3-7	Gravity	264	84	7035557	568157
0707004	4-7	Gravity	225	97	7035746	568269
0707005	5-7	Gravity	192	62	7035433	569127
0707007	7-7	Gravity	242	67	7036916	570741
0707009	9-7	Gravity	230	66	7036875	570854
GS08-157-06PC	GS08	Piston	1443	67	7035453	568532

Logger (MSCL; Geotek Limited, Daventry, Northants, UK) at Sedimentlaboratoriet, Department of Earth Science, University of Bergen. The results were used to identify general grain-size variations. Twelve samples were impregnated with epoxy and prepared for thin sections at the Department of Geography, Royal Holloway, University of London, for a microscope study of grain-size variations, grain fabric, sorting, sedimentary structures and mineralogy within specific facies (for example, within FA4). Coarse silt grains may be identified under the microscope, whereas finer mud usually appears as a massive matrix. A few samples were dried and prepared for analysis through scanning electron microscopy (SEM) using the dry-fracture-peel/blow procedures (Mitchell, 1993) for a closer examination of grain shapes and grain fabric in the most fine-grained facies. Mineral characterization was done by X-ray diffractrometry or grain counting under the microscope. One long core (GS08) was chemically characterized through X-ray fluorescence using an ITRAX Core Scanner (Cox Analytical Systems, Molndal, Sweden) at Sedimentlaboratoriet, Department of Earth Science, University of Bergen. Water content and bulk density were calculated by drying and weighing samples with a known volume. Contents of total organic carbon (TOC) were also analysed using a Leco oven (Leco Corporation, St. Joseph, MI, USA). Undrained shear strength was measured at 5 to 10 cm intervals using the Swedish Fall cone.

Terminology

The term 'clays' or 'clay deposits' is applied as a general description of unconsolidated, muddy (glacio) marine deposits on land as found in Canada, Norway and Sweden (e.g. Rosenqvist, 1966; La Rochelle *et al.*, 1970; Karlsrud *et al.*, 1985; Lefebvre, 1996), although the content of silt can be significant. For the description of cores, 'mud' is considered as a mixture of clay and silt, whereas sandy mud contains <50% sand (Flemming, 2000). The Udden-Wentwoorth scale (Friedman & Sanders, 1978) is applied for detailed description of grain sizes. The term 'clay-rich' is applied for sediment that is relatively enriched in clay-sized material compared with the surrounding deposit. For detailed facies analysis, 'lamination' refers to layers with thicknesses on a grain scale to millimetre scale within beds. 'Beds' have thicknesses on a centimetre scale or more. The term 'stratification' is used more generally and includes both bedding and lamination.

Radiocarbon dating

Remains of mollusc shells were identified on species level and radiocarbon dated using accelerator mass spectrometry at the National Laboratory for Radiocarbon Dating at NTNU, Norway (TUa samples) and Poznan Radiocarbon Laboratory, Adam Mickiewicz University, Poznan, Poland (Poz samples). Results are summarized in Table 2. Calibration has been carried out (Stuiver & Reimer, 1987; Bronk Ramsey, 2001; Hughen *et al.*, 2004) with a reservoir correction value ΔR of -3 ± 22 as estimated for southern Norway (Mangerud *et al.*, 2006). The ages of event beds are assessed preferentially on the basis of dates obtained from samples taken closely below their base. Dating of reworked mollusc shells within a gravity-flow deposit helps

Table 2. AMS ^{14}C dates obtained from mollusc shells in cores.

Laboratory number and sample number	Abbreviated core number	Year of dating	Depth in core (cm)	Water depth (m)	Species of dated mollusc shells	Facies association (FA)	^{14}C age BP Reservoir corr. 440 years	(1) Calibrated age BP (BP = 1950) 1σ range	(2) Calibrated age BP (BP = 1950) 1σ range	Delta ^{13}C (0/00) VPDB
TUa-7496 0601009-2-027	9	2008	130	105	*Abra alba/nitida*?	2	1595 ± 40	1620–1525	**1670–1540**	−0·8
TUa-7495 0601012-2-039	12	2008	134	91	*Abra alba*	2	2025 ± 40	2135–2025	**2190–2030**	−0·1
TUa-7492 0601013-2-002	13	2008	69	90	*Abra alba*	2	2815 ± 40	3125–2980	**3170–3010**	1·5
TUa-7494 0701003a-168	3–1	2008	168	84	*Abra alba*	4	3430 ± 40	3865–3730	**3920–3760**	−1·7
TUa-7493 0701003a-185	3–1	2008	185	84	*Abra alba*	4	3260 ± 40	3640–3540	**3690–3550**	−2·7
TUa7334 0707004-1-070	4–7	2008	70	97	*Pseudamassium septemradiatum*	2	4255 ± 30	4950–4840	**4970–4850**	3·9
TUa7333 0707004-2-025	4–7	2008	130	97	*Antalis* sp.?	2	4855 ± 35	5685–5595	**5700–5600**	1·9
TUa-7497 0707005-2-064	5–7	2008	154	62	*Abra nitida*	4	1435 ± 35	1450–1340	**1490–1360**	−4·6
TUa-6336 0601004-081	4	2007	81	110	*Pseudamassium septemradiatum*	2	2080 ± 35	2245–2110	**2300–2170**	2·8
TUa-6335 0601004-081	4	2007	25	110	*Antalis*	2	245 ± 35	335–275	**390–280**	1·8
TUa-7775 GS08-A076	GS08	2009	76	67	*Abra alba*	3	1360 ± 35	**1355–1280**	–	0·5
TUa-7711 GS08-A102	GS08	2009	102	67	Shell fragments	2	1415 ± 40	**1415–1320**	–	1·0*
TUa-7776 GS08-B1005	GS08	2009	122	67	*Littorina littorea*	2	1550 ± 40	**1565–1485**	–	2·7
TUa-7777 GS08-B1036	GS08	2009	153	67	*Abra alba*	2	1625 ± 40	**1680–1550**	–	1·0

Table 2. (Continued)

Laboratory number and sample number	Abbreviated core number	Year of dating	Depth in core (cm)	Water depth (m)	Species of dated mollusc shells	Facies association (FA)	^{14}C age BP Reservoir corr. 440 years	(1) Calibrated age BP (BP = 1950) 1σ range	(2) Calibrated age BP (BP = 1950) 1σ range	Delta ^{13}C (0/00) VPDB
TUa-8134 GS08-B2028	GS08	2009	191	67	*Abra nitida*	2	1600 ± 35	**1630–1530**	–	1·0*
TUa-7712 GS08-B3014	GS08	2009	207	67	*Pseudamassium septemradiatum*	2	1710 ± 35	**1770–1675**	–	2·9
TUa-7778 GS08-B3030	GS08	2009	228	67	*Arctica Islandia*?	2	1775 ± 40	**1850–1730**	–	1·0*
TUa-7713 GS08-B3072	GS08	2009	265	67	*Abra*?	2	2085 ± 35	**2260–2115**	–	1·0*
TUa-7779 GS08-C072	GS08	2009	344	67	*Abra alba*	2	2675 ± 40	**2925–2805**	–	1·3
TUa-7714 GS08-C121	GS08	2009	387	67	*Nuculoma tenuis*	2	2960 ± 40	**3320–3200**	–	1·0*
TUa-7780 GS08-C134	GS08	2009	406	67	*Abra alba*	2	2870 ± 40	**3205–3070**	–	1·2
TUa-7781 GS08-D024	GS08	2009	433	67	Unknown	3/4	2910 ± 40	**3250–3130**	–	3·3
TUa-7715 GS08-D119	GS08	2009	525	67	*Abra alba*	3/4	3475 ± 35	**3915–3820**	–	0·5
TUa-8135 GS08-F1015	GS08	2009	724	67	*Abra alba*	2	3295 ± 30	**3685–3590**	–	0·5
TUa-7716 GS08-G053	GS08	2009	904	67	*Glossus humanus*	4	4020 ± 40	**4690–4530**	–	3·0
TUa-7782 GS08-I029	GS08	2009	1178	67	*Tracia* sp.	2	5280 ± 40	**6180–6065**	–	3·6

The values in bold indicate the ages used in this study. Detailed information about other relevant dates used in this study is presented in L'Heureux *et al.* (2009). (1) Calibrated age (Stuiver & Reimer, 1987), (2) Calibrated age (Bronk Ramsey, 2001; Hughen *et al.*, 2004) with a reservoir correction value ΔR of −3 ± 22 (for southern Norway, Mangerud *et al.*, 2006).
Uncertain species identifications are marked with ?. Estimated Delta ^{13}C values are marked with *.

to give a maximum age for the deposit. It has to be taken into consideration that some of the dated molluscs are burrowing organisms (for example, *Abra alba*) whereas others live on the sea bed (for example, *Pseudamussium septemradiatum*). A few mollusc shells are reworked. Considering the above uncertainties, the ages of event beds are only indicative. Sediment reworking and the presence of hiati in the stratigraphy mean that accurate sediment accumulation rates are difficult to determine within the cores.

SEDIMENTOLOGY

The fjord-marine deposits in the bay of Trondheim have been divided into four main facies associations (FA1 to FA4) based on visual descriptions (Figs 2 to 7). FA1 to FA3 are generally described as a facies continuum whereas FA4 is divided into five discrete facies types aided by thin-section analysis (Figs 8 and 9). Transitions between the different facies associations are present.

Mineralogy

Mineral analysis reveals that all facies contain quartz, plagioclase, mica (muscovite, biotite and maybe illite), chlorite and amphibole. Calcareous material is also present. The analysis also indicates that clay-rich facies within some beds of FA3/FA4 contain a higher amount of mica relative to chlorite when compared with the surrounding, bioturbated sediments of FA2.

Facies Association 1 (FA1): Sand and gravel

Description

Facies Association 1 consists of poorly sorted, matrix-supported to clast-supported sand and gravel. The beds are up to 20 cm thick and commonly dominate the upper 50 cm of cores (Figs 2 to 4). One core from near land is entirely dominated by FA1 (Core 1-1; Fig. 4). Fragments of mollusc shells, wood, slag or other anthropogenic material are present. Due to the coarse grain sizes, the density is relatively high and the magnetic susceptibility varies significantly due to a varying mineral composition (for example, Fig. 2).

Interpretation

Facies Association 1 is interpreted primarily as having been deposited from sandy to gravelly sediment gravity flows combined with anthropogenic drop of building materials, plastic and slag. Littoral to sublittoral wave and current processes possibly also affected the thicker beds of sand in Core 1-1 (Fig. 4). Winnowing may locally have played a role in the concentration of coarser sediments elsewhere on the sea bed.

Facies Association 2 (FA2): Bioturbated mud to sandy mud

Description

Facies Association 2 consists of structureless to mottled or weakly stratified, brownish-grey, mud to sandy mud. Mean grain sizes vary from 20 to 50 μm based on Coulter counting. The clay content varies but is relatively low (Fig. 2). Accumulations of this dominating facies association can be several metres thick. At deeper stratigraphic levels, grain sizes are slightly finer (Core GS08, Fig. 3). However, there are several, smaller, superimposed changes in grain size throughout the core as shown by both visual descriptions and logs (Figs 3 and 4). Small-scale, soft-sediment deformation structures are present (for example, Fig. 8B), and thin sections display a random orientation of grains. Less than 10 cm thick, diffuse layers or lenses of greyish, finer-grained sediments are present locally as shown by crosses in the logs (for example, Figs 2 and 3). Less than 4 cm thick beds of well-sorted fine sand and/or medium sand are also marked. Some of these thin sand beds are found at the base of FA2 overlying FA4 (Cores 3-1 and 13; Fig. 4). Here, inversely graded very fine sand to coarse sand with angular clasts, and a slightly imbricated fabric, is observed (Fig. 8A). A few dropstones or pieces of wood are present in a few cores. Typical values for water contents and shear strengths are 25 to 35% and 7 to 20 kPa, respectively (Fig. 2). Total organic carbon typically varies between 0·2% and 0·5% (Fig. 3), with locally higher values. Mollusc shells of, for example, *Abra alba* and *Pseudamussium septemradiatum* are common (Table 2). The first mentioned deposit feeder is tolerant of high sedimentation rates, whereas the latter is a suspension-feeding organism. A few mollusc shells are reworked, such as one recorded shell of *Mytilus edulis* that usually lives in water depths of <20 m.

Interpretation

The deposits of FA2 are interpreted as fjord-marine sediments. Bioturbation has destroyed most of the primary sedimentary features, thus inhibiting a detailed interpretation of the sedimentation processes. However, the weakly

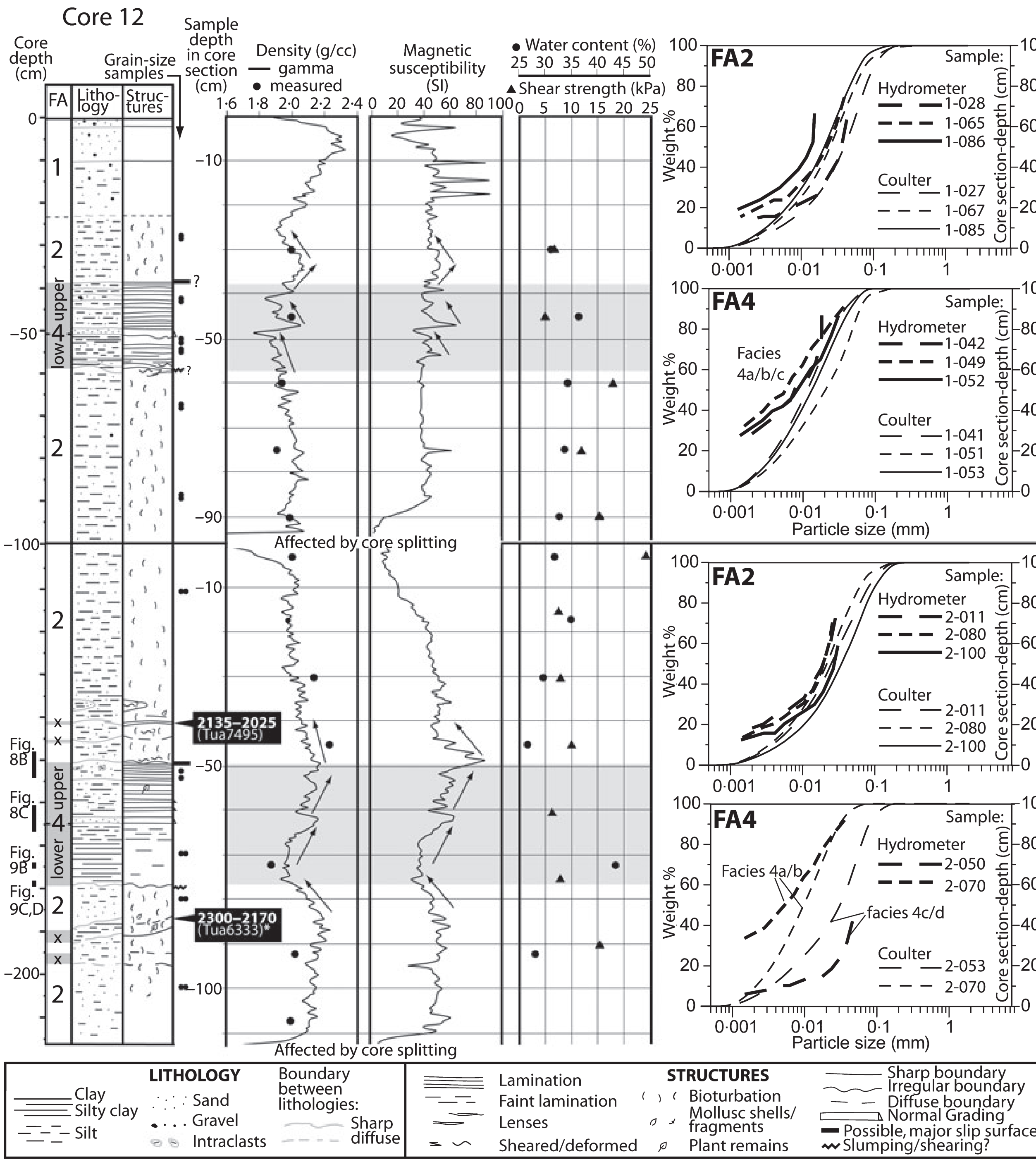

Fig. 2. Sedimentological log for Core 12 sampled at 91 m water depth (see Fig. 1D for sample location). Thin, greyish, fine-grained beds in FA2 are indicated by an 'x'. Data on density, magnetic susceptibility, water content, shear strength and grain size from hydrometer testing (wt %) and Coulter counting (vol %) are presented. Main grain-size trends are indicated with arrows. Radiocarbon dates are shown in cal yr BP (white text on black background). The date indicated by an asterisk (*) is from L'Heureux *et al.* (2009). Selected sample locations for thin sections are indicated with reference to figures where details are shown.

stratified appearance indicates a combination of common fjord-marine processes such as hemi-pelagic sedimentation, and deposition from currents and/or smaller-scale sediment gravity flows. The latter is supported by the presence of thin sand beds, including thin, inversely graded beds that are probably the result of grain flows (e.g. Middleton & Hampton, 1973). Soft-sediment

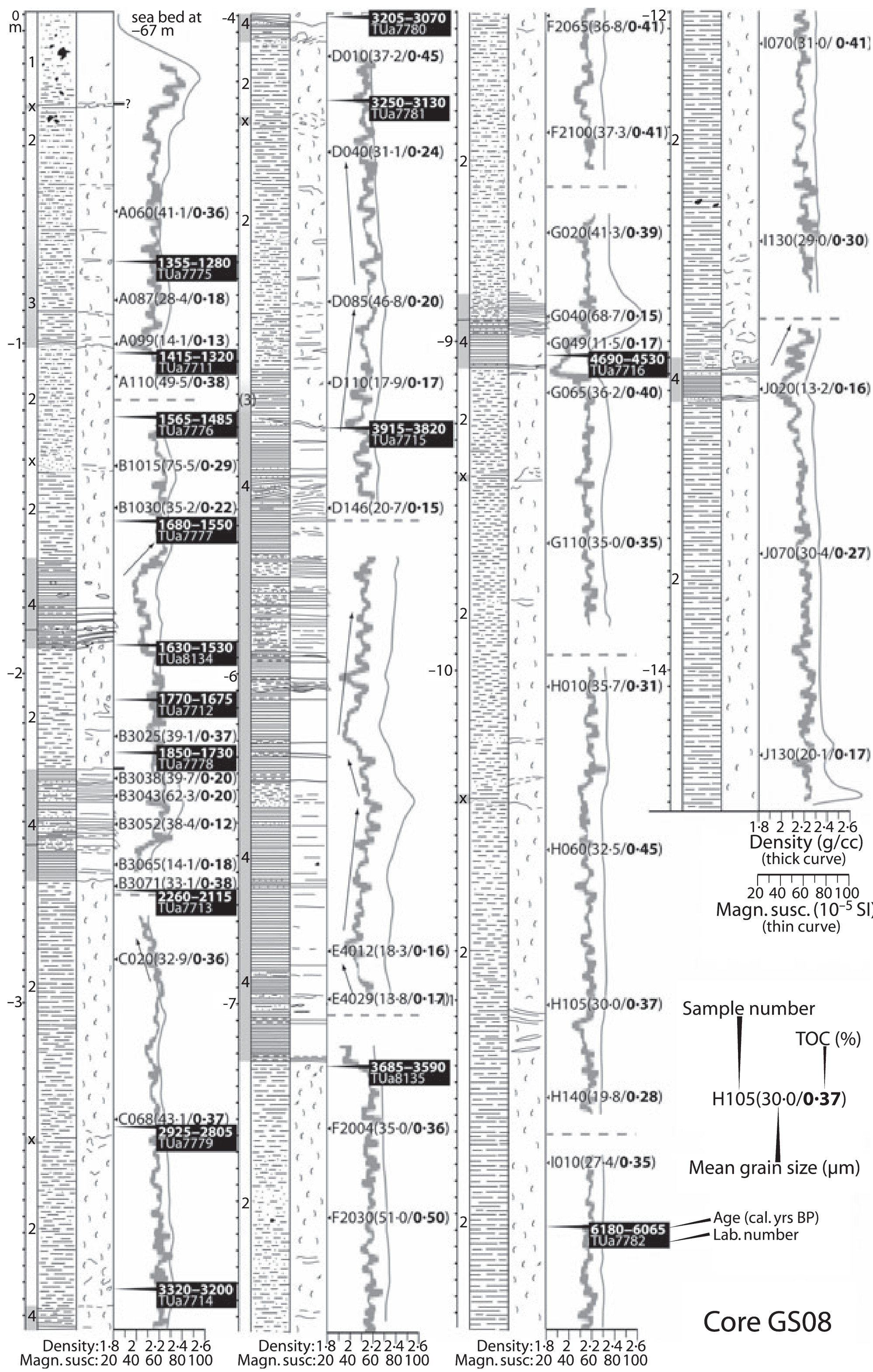

Fig. 3. Sedimentological log for Core GS08. Levels of core splitting are indicated with stippled lines. Facies associations are indicated in the left column. Thin, greyish, fine-grained beds in FA2 and one thin, sand bed at 135 cm, are indicated by an 'x'. Radiocarbon dates are shown in cal yr BP. Grain-size analyses from Coulter are also indicated (mean grain size in μm) in parentheses together with TOC values in bold (%). A few general grain-size trends from density and magnetic susceptibility logs are indicated with arrows. For location of core, see Fig. 1D. For legend, see Fig. 2.

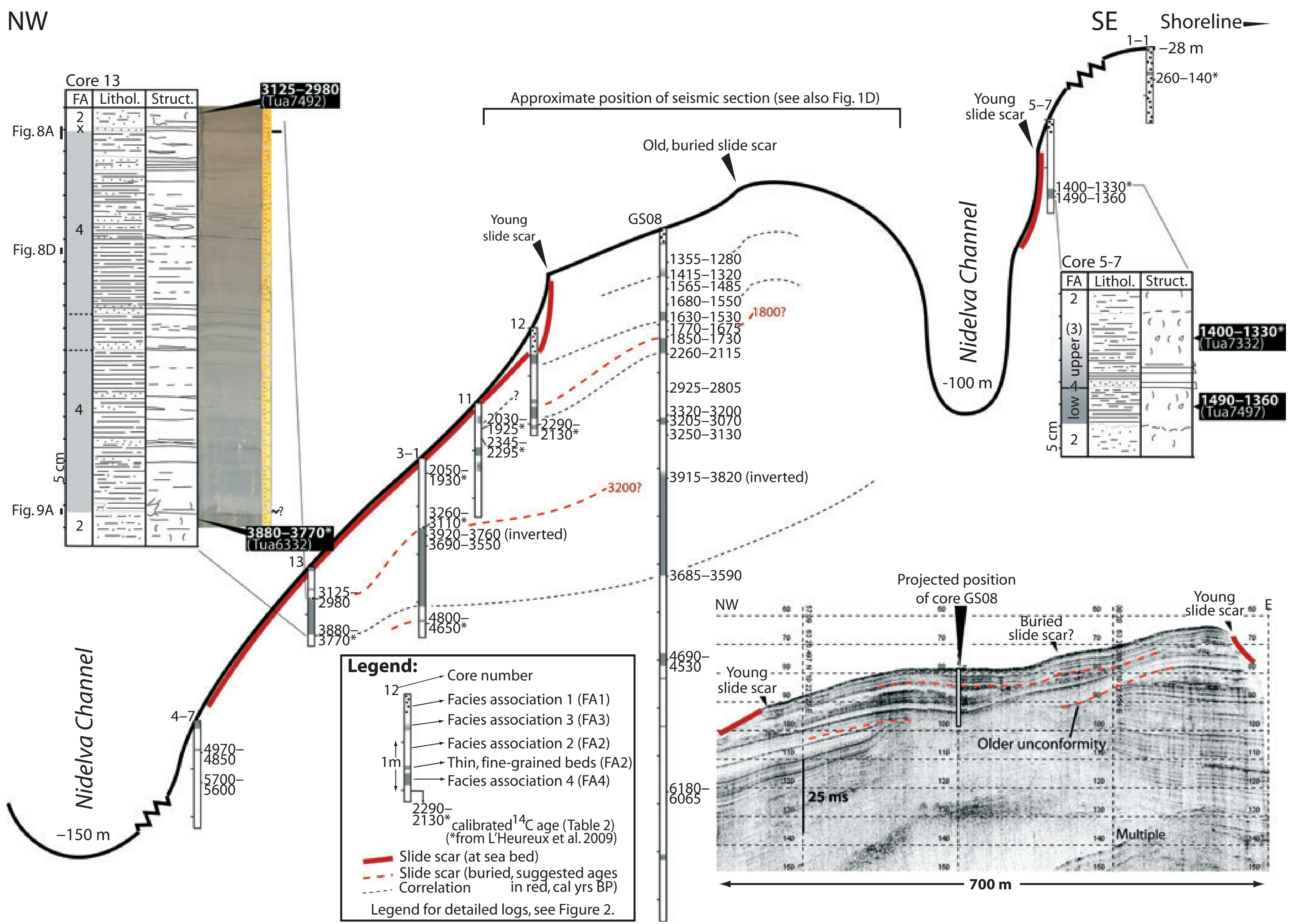

Fig. 4. Schematic NNW to SSE trending transect displaying the main morphological elements (slide scars, Nidelva Channel) and the distribution of clay-rich beds in selected cores. For the location of cores, transect and seismic section, see Fig. 1D. The transect is not to scale, but some characteristic depths, for example, of the Nidelva Channel, are indicated. Legend for detailed logs, see Fig. 2. Detailed log for GS08 is shown in Fig. 3. Cores are correlated on the basis of radiocarbon dates, characteristics of clay-rich beds and their bounding surfaces. The seismic section displays a few unconformities interpreted as buried slide scars. The upper part of Core 11 may contain landslide debris.

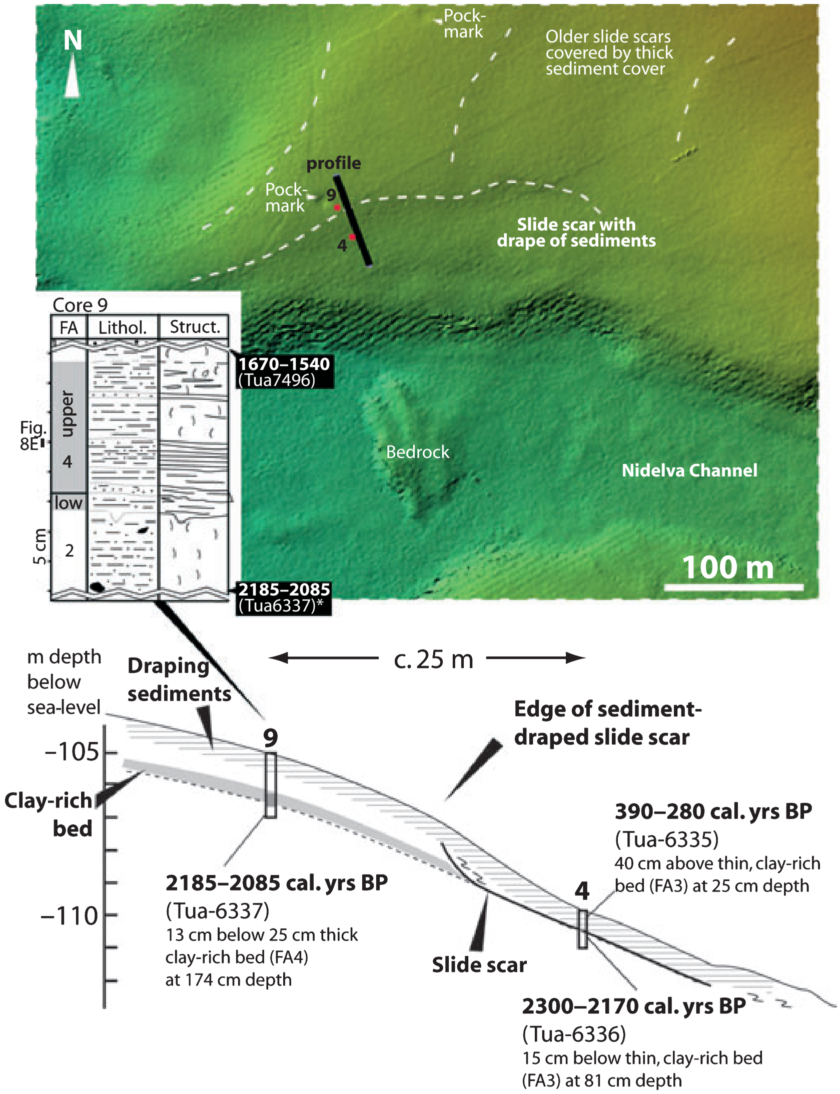

Fig. 5. Old slide scar north of the Nidelva Channel with radiocarbon-dated cores. Other, older slide scars and pockmarks are shown. The profile indicates that the sediment-draped slide scar north of the Nidelva Channel follows the position of the clay-rich bed in Core 9. For position of map, see Fig. 1D.

deformation structures and lenses support the activity of resedimentation processes. Thin, fine-grained, greyish beds record an occasional increase in the input of finer sediments. However, some thin beds possibly reflect deformation or erosion of thicker accumulations of FA3 or FA4 (see later section). Dropstones were transported by sea ice or drift wood. Core GS08 (Fig. 3) displays an overall upward coarsening tendency within FA2; this is explained by an overall shallowing and progradation of the shoreline during a fall of relative sea-level in the Holocene (L'Heureux *et al.*, 2009). Smaller-scale grain-size variations are explained by changes in sediment supply and prevailing processes. Facies Association 2 is considered as representing the range of processes occurring under 'normal' conditions with sedimentation rates that are, on average, low enough to allow for biological activity disturbing most of the sedimentary structures.

Facies Association 3 (FA3): Grey, bioturbated, clay-rich mud with little sand

Description

Facies Association 3 consists of a bioturbated to weakly stratified mud with a distinct light-grey colour, a few minor shell fragments and millimetre-sized black stains of organic material. A few centimetre-thick sandy layers are present locally. Coulter analysis shows a mean grain size of 8 to 16 μm locally increasing slightly upwards (for example, at 1 m in Core GS08; Fig. 3). Accumulations are 50 cm to more than 180 cm in thickness (for example, in Cores 3-7, 7-7, 9-7; Fig. 1D). The lower boundary was only exposed in

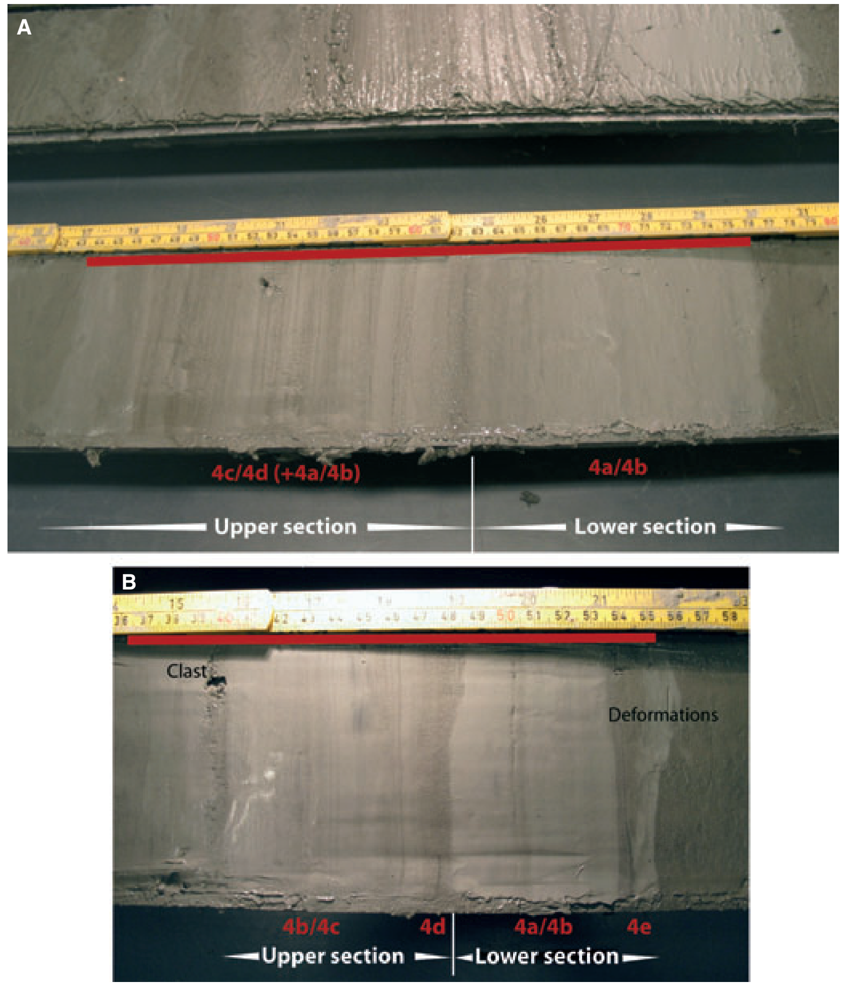

Fig. 6. Photographs of stratified, clay-rich event beds (FA4). The beds are marked with a red line and facies are indicated with red letters. Note the difference between the lower (generally finer-grained) and the upper sections (generally more sandy). The dominant facies are indicated. (A) Event bed at 50 cm depth in Core 12, see log in Fig. 2. Both the lower and the upper divisions display general upward-coarsening tendencies. (B) Event bed at 160 cm depth in Core 12, see log in Fig. 2. Both the lower and the upper divisions display general upward-fining tendencies. Note the deformations at the base. Lower scales are in centimetres.

one core (at 1 m in Core GS08, Fig. 3), displaying a lower sharp boundary of a 50 cm thick bed. The upper boundary usually is gradational or locally affected by deformation structures. Facies Association 3 is, in some cases, identified at the upward transition from FA4 to FA2 (for example, at 5 m in Core GS08; Fig. 3). Total organic carbon is relatively low, typically between 0·15% and 0·25%. The measured shear strength varies but tends to be lower than the surrounding sediments; this is exemplified in Core 3-7 where values in FA3 were lower (<10 kPa) than for the overlying bed of FA2 (10 to 30 kPa).

Interpretation

Bioturbation within FA3 has disturbed the primary sedimentary features, limiting a detailed interpretation of the sedimentation processes. The generally fine grain size indicates a high supply of mud. As for FA2, deposition is interpreted as a result of a combination of processes including suspension sedimentation and/or deposition from various types of sediment-gravity flows. The latter gave rise to the intercalated sandy layers, which testify to occasionally higher sedimentation rates. Thicker accumulations of FA3 must have been deposited over a period of time, semi-continuously and/or in pulses, as average sedimentation rates were low enough to allow for intermittent biological activity. The preserved, sharp lower boundary of the 50 cm thick bed is explained by an initially rapid deposition of a clay-rich bed that was sufficiently thick so that the subsequent biological activity did not destroy its lower boundary. It follows that, at any given location, the preservation of primary sedimentary structures will depend on the overall sedimentation rates compared with the intensity and depth of bioturbation. Facies Association 3 is regarded as a lateral to distal equivalent of FA4 described below and is transitional to FA2.

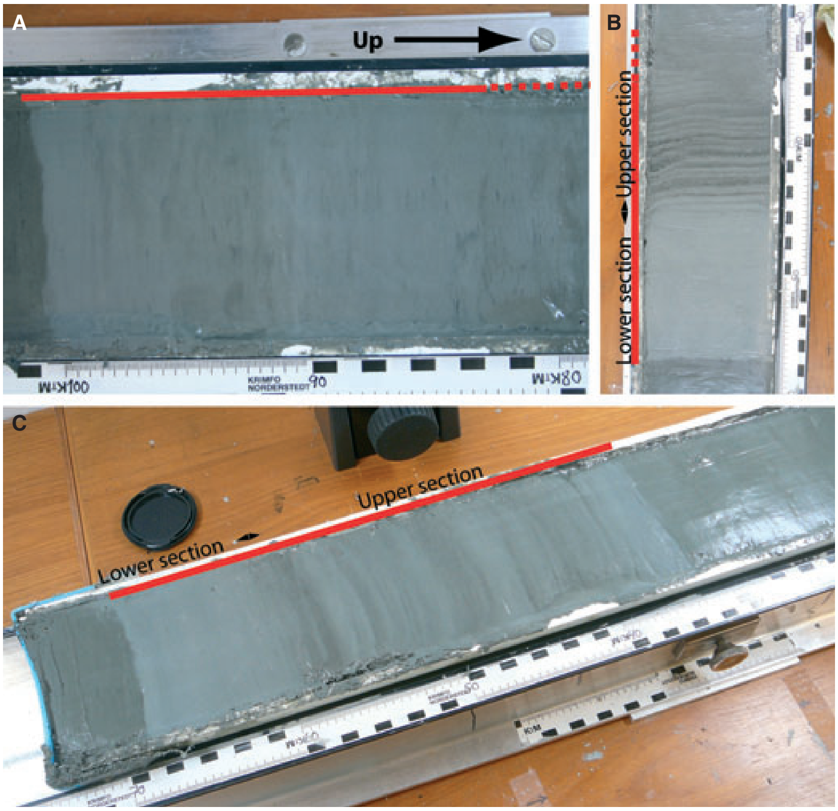

Fig. 7. Photographs of clay-rich event beds in Core GS08 (Fig. 3). The beds are marked with a red line. (A) Bioturbated clay-rich bed with sharp lower boundary at 1 m depth (FA3). (B) Stratified clay-rich bed with partially bioturbated top (FA4) at 9 m depth. (C) Stratified clay-rich bed (FA4) at 2·5 m depth. Note that both the lower and upper boundaries appear sharp. Note the clear division into a finer-grained lower section and a more sandy upper section in both (B) and (C). Scales are in centimetres.

Facies Association 4 (FA4): Grey, stratified, clay-rich mud with little sand

Description

Facies Association 4 has a distinct light-grey colour and is clearly stratified with several facies containing clay, silt and/or very fine sand. The clay content is relatively high and hydrometer testing shows that it generally varies from 30 to 37% in the finer-grained parts to only 5% in the coarser-grained parts (Fig. 2). For comparison, Coulter counting usually gives a mean grain size of 11 to 20 μm in the finer-grained parts whereas samples reach up to 70 μm in the coarser-grained parts, usually near the tops of the beds (Core GS08; Fig. 3). The marked differences between the two applied methods are explained by a high content of platy grains such as mica and differences in the techniques used (Syvitski *et al.*, 1991; Cramp *et al.*, 1997). A high content of mica is supported by thin-section analysis and counting of mineral grains in the silt and fine sand fractions, giving over 20% of mica in one sample. Density and magnetic susceptibility logs reflect the varying grain sizes (Figs 2 and 3). The colour is ascribed to a low content of organic material, as shown from TOC values of typically 0·1 to 0·2% from the finer-grained facies, combined with a high clay content, as reflected by X-ray.

Facies Association 4 is divided into five interbedded facies (Facies 4a to 4e) and each bed is <5 cm in thickness: *Facies 4a* – Structureless to wispy silt in mud of diverse sorting and a varying content of coarse silt in a mud matrix (Figs 8A, 8C and 9). Boundaries between poorly sorted and sorted parts are diffuse. Millimetre-sized wisps or streaks of silt grains give rise to a weak stratification locally and diffuse millimetre-sized trough-shaped features have been observed. *Facies 4b* – Diffusely laminated to graded couplets in silt and mud with poor sorting (Fig. 8C and E). Load casts have been recorded. *Facies 4c* – Distinctly laminated mud to very fine sand with a matrix of mud (Fig. 8C and D). A few poorly sorted, millimetre-sized silt lenses are present, locally with rippled tops and/or a poorly developed ripple lamination. *Facies 4d* – Structureless to faintly laminated silt to very fine sand, with a low content of mud (Fig. 8B and C). The beds commonly display an irregular, erosional, loaded and/or deformed base. Some structureless beds contain intraclasts of mud. *Facies 4e* – Irregularly bedded, poorly sorted mud with some sand and biogenic remains (Fig. 9A and C). Inclusions of more well-sorted silt are present. This facies is recorded in a few

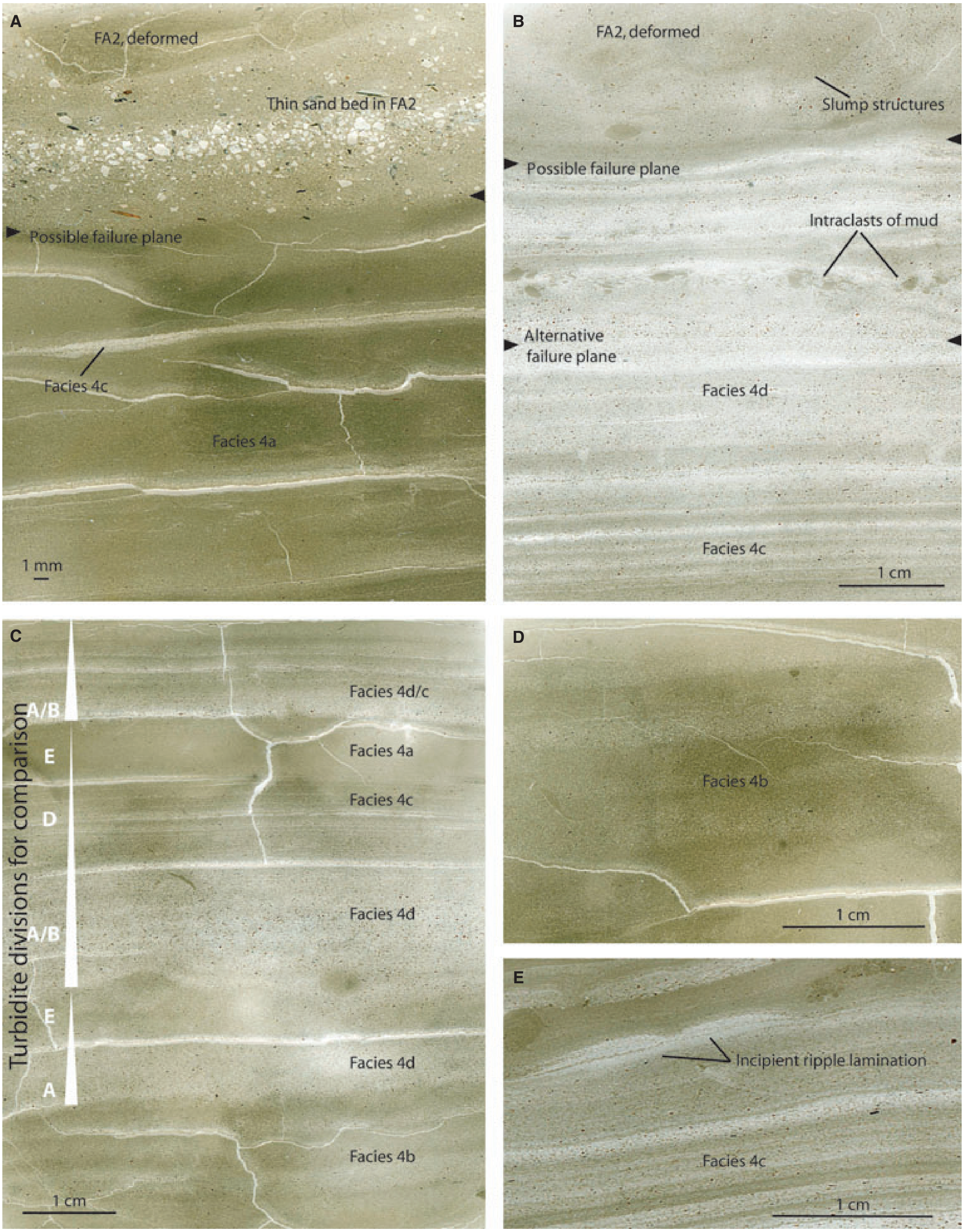

Fig. 8. Details from thin sections showing typical facies from the stratified, clay-rich beds of FA4. (A) Top of FA4 in Core 13 (Fig. 4). (B) Top of stratified clay-rich bed in Core 12 (at 150 cm; Fig. 2). (C) Stacked turbidites in stratified clay-rich bed in Core 12 (at 160 cm; Fig. 2). Divisions of (silt) turbidites (*sensu* Stow & Piper, 1984; Bouma, 1962) are indicated for comparison. (D) Detail from the uppermost part of Core 13 (Fig. 4). (E) Detail from Core 9 (Fig. 5).

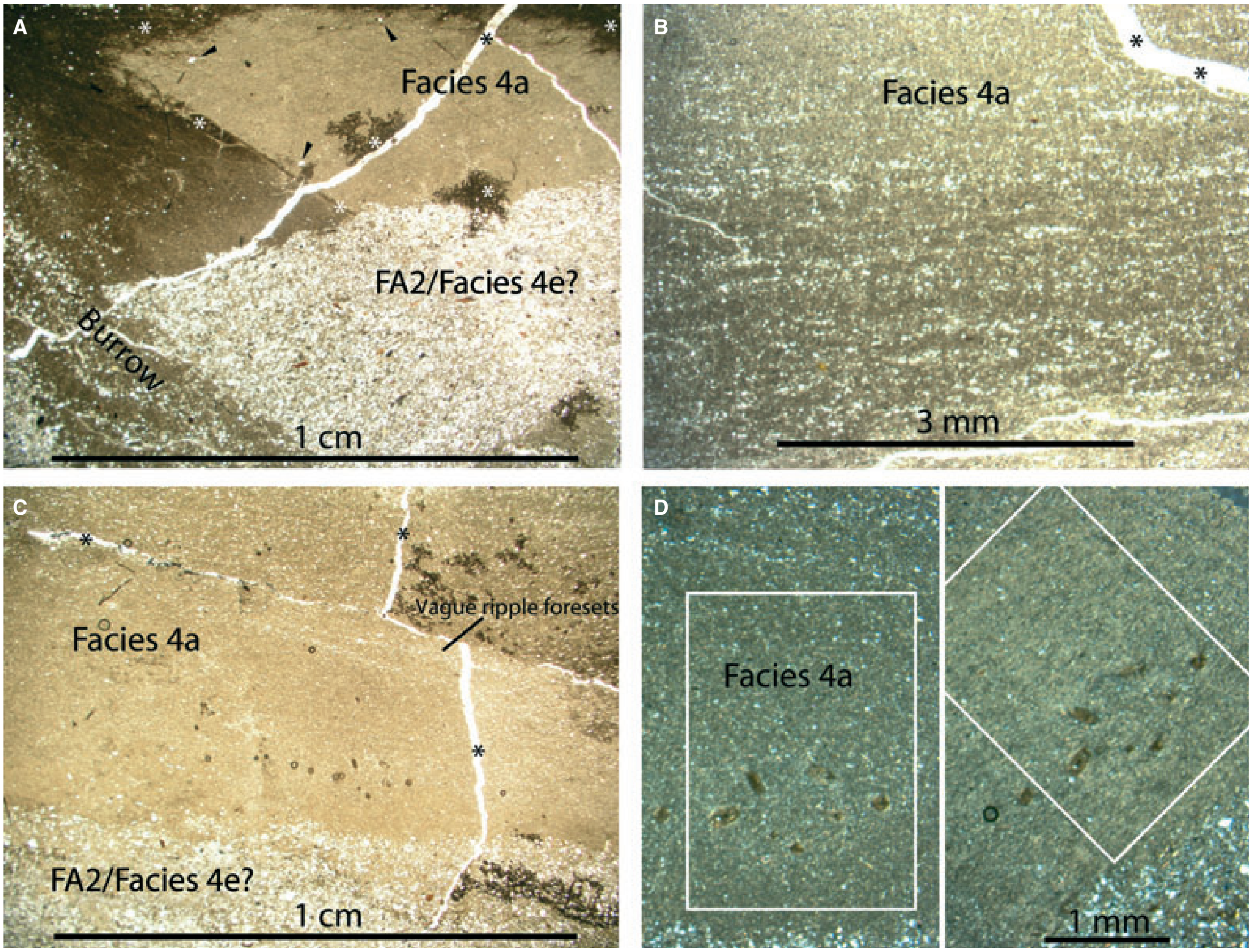

Fig. 9. Details from thin sections of facies in stratified clay-rich beds (FA4). Artifacts from the preparation of thin sections are marked with an asterisk (*). (A) Detail from the lowermost part of the clay-rich bed in Core 13 (Fig. 4). Note the few, larger silt grains in otherwise structureless mud. (B) Poorly sorted mud with streaks of silt. Detail of lower part of FA4 in Core 12 (at *ca* 175 cm; Fig. 2). (C) Detail from the base of clay-rich bed in Core 12 (at *ca* 180 cm; Fig. 2). (D) Detail of (C) in polarized light. Note the uniform extinction pattern of the sediment that testifies to a preferred orientation of platy minerals parallel to bedding.

cores at the lower boundary above FA2. Except for a slightly higher sand content, this facies is difficult to distinguish from FA2.

The more fine-grained, well-sorted mud facies display a relatively well-defined orientation of mica parallel to bedding. This effect is shown by the optical extinction pattern in polarized light seen in thin sections (Fig. 9D). The more poorly sorted facies generally display a more poorly developed grain orientation with angular, equant to platy grains in a matrix of mud. Silty to sandy beds display a packing of angular, equant and platy grains usually with a matrix of mud. Scanning electron microscopy analysis from Facies 4a (4b) shows angular grains of, for example, quartz, feldspars and mica in a matrix of clay with thin, commonly single, plate-like particles (*sensu* Bennett *et al.*, 1981; Fig. 10). The particle arrangement locally displays an open honeycomb structure (*sensu* Sergeyev *et al.*, 1980; Fig. 10).

The lower boundary of FA4 appears sharp and slightly undulating, representing an abrupt lithological change from the brownish deposits of FA2 to the light-grey deposits of FA4. However, in some cases, the lowermost centimetre of FA4 is slightly sandy and can then be identified as Facies 4e or, in a few cases, as a thin version of Facies 4c or 4d. Facies Association 4 is found in two versions distinguished by thickness and internal organization. The 'typical' beds are usually 15 to 25 cm thick and are divided into a lower, clay-rich section dominated by Facies 4a and 4b, sharply overlain by an upper section, which is slightly sandier and dominated by

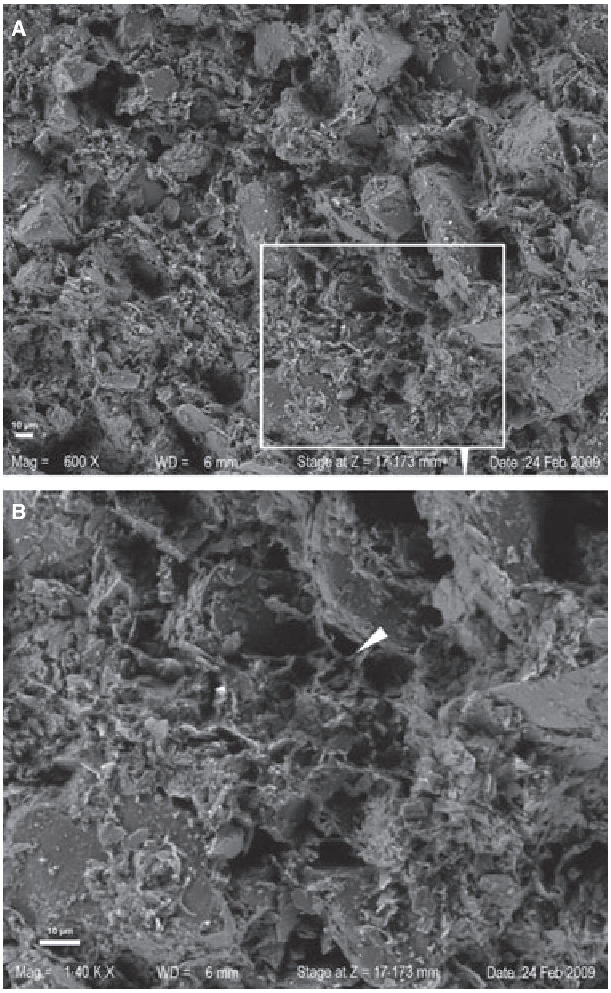

Fig. 10. SEM images of Facies 4a or 4b. Note the open structure and poor sorting with angular clasts of silt, numerous plate-like grains and areas with an open 'honeycomb' fabric of clay particles (for example, at the arrow).

Facies 4b, 4c and 4d (Figs 6, 7B and 7C). However, several trends of grading may be present within the lower and the upper sections (for example, Figs 2 and 6). A few 'atypical' beds are significantly thicker and reach up to 85 to 200 cm, for example, in Cores 13, 3-1 and GS08 (Figs 3 and 4). These thick beds are not so easily divided into lower and upper sections and display several overall trends in grading (for example, Fig. 3; see also L'Heureux *et al.*, 2009). The upper boundary of FA4 either is gradual and marked by bioturbation, or is sharp and locally overlain by 1 to 1·5 cm thick sand beds within FA2. Bioturbation is observed locally, as well as a few, millimetre-sized black stains of organic material. Mollusc shells of *Abra alba*, *Abra nitida*, *Glossus humanus* and *Mytilus edulis* have been recorded in the beds. Measured water contents are relatively high and values of 38 to 45% have been recorded in the more fine-grained facies in Core 12 (Fig. 2). Measured shear strength is generally lower than for the surrounding facies associations, as exemplified in Core 12 where values are 5 to 10 kPa, compared with 7 to 20 kPa for FA2 (Fig. 2).

Interpretation

Facies Association 4 is interpreted as deposited by a combination of traction and suspension fallout and facies are comparable with the divisions of (silt) turbidites (*sensu* Stow & Piper, 1984; Bouma, 1962; Fig. 8C). The structureless to faintly laminated silt and very fine sand (Facies 4d) was deposited through rapid dropout from suspension with some influence from traction. The distinctly laminated mud to very fine sand (Facies 4c) was deposited by pulsating flows with a well-developed shear sorting of silt and clay in the bottom boundary layer (*sensu* Stow & Bowen, 1980). The diffusely laminated to graded couplets in silt and mud (Facies 4b) were deposited through a combination of suspension fallout of flocs and silt grains from slightly pulsating flows with high suspension concentrations, and possibly with some shear sorting of silt and clay in the bottom boundary layer (*sensu* Stow & Bowen, 1980). Lamination can also have formed by fluctuating transitional flows (Baas & Best, 2002). The structureless to wispy silt in mud of diverse sorting (Facies 4a) reflects a contemporaneous suspension fallout of flocs and silt grains giving rise to poor segregation of grain sizes (for example, Kranck, 1984). The poorest sorting was promoted by high clay concentrations and associated with reduced turbulence, whereas increasing turbulence and shear in more diluted flows reduces floc size (Baas & Best, 2008). Suspension sedimentation, however, was accompanied by some traction giving rise to wisps of silt, trough-shaped features and poorly developed ripple foresets in silt (Fig. 9B and C). Floccule ripples (*sensu* Scheiber *et al.*, 2007) may have formed locally, although high contents of suspended clay possibly inhibited ripple formation (e.g. Baas & Best, 2002). In cases of very high clay concentrations, such as in the beginning of a flow, floc settling rates can even have exceeded the settling rates of single grains (Kranck, 1984). This process could explain the presence of some relatively well-sorted layers in Facies 4a with a few floating grains, for example, at the base of FA4 (Fig. 9A, C and D). Structureless to faintly laminated silt and very fine sand (Facies 4e) is interpreted as the product of deformation, slumping and/or shear-

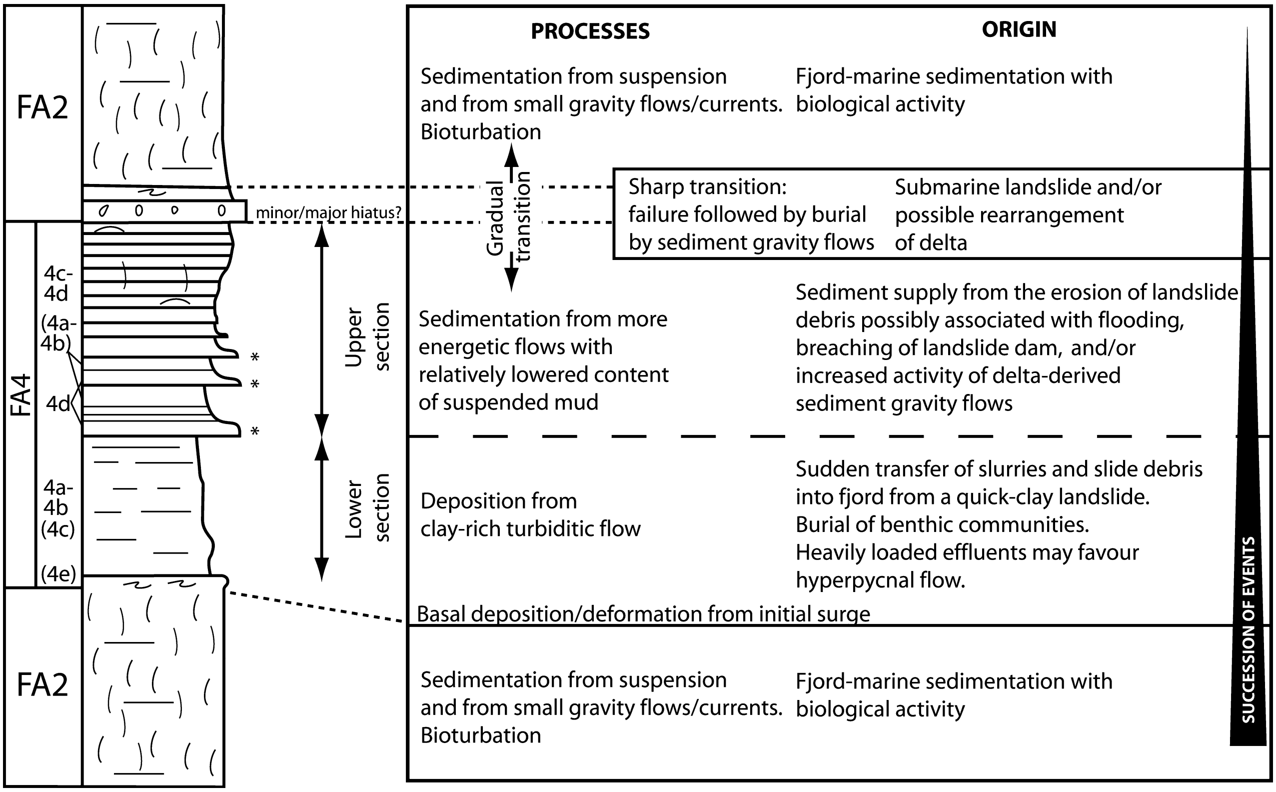

Fig. 11. Synthesis of sedimentation processes and origin of the typical, stratified, clay-rich beds. Facies associations and dominating facies for FA4 are indicated. Potential, erosional intrabed-contacts are indicated by an asterisk (*).

ing beneath a sediment gravity flow. During this process, the sediments became mixed with FA2 below, possibly aided by escaping organisms.

In general, the stratified, clay-rich beds of FA4 are interpreted as deposited (semi-continuously) from turbiditic clay-rich flows of varying strength and suspended concentration (Fig. 11). A major part of the flow activity possibly passed into the Nidelva Channel (Fig. 1D). Facies Association 4 represents the spill over from these flows (L'Heureux *et al.*, 2009) and is regarded as base-cut-out turbidites (e.g. Stow & Piper, 1984). The abrupt change in sediment properties from FA2 to FA4 shows that deposition was fast and represents a sudden event. The biological activity was reduced primarily due to high sedimentation rates and high turbidity. Thus, the primary sedimentary features are preserved. There are also traces of organisms that tried to escape. The presence of a relatively thick mud bed (primarily Facies 4a and 4b) overlying a thin sandy bed (Facies 4c, 4d or 4e) or FA2 implies the passage of a flow with a high proportion of clay-sized material (Stow & Piper, 1984). The poor development of a sandy/silty base can be explained by drag reduction beneath viscous, clay-rich flows (*sensu* Baas & Best, 2008), by which centimetre-sized shell fragments, such as *Mytilus edulis*, could be transported. The 'typical' upward change to a more sandy section within FA4 reflects a lowering in the content of fines and/or increased turbulence and flow power associated with additional sand and silt. This trend can, in some cases, reflect a development within a single flow. However, the overall grain-size trends, for example, with two superimposed normal graded sections shown in Fig. 6B indicate that, in this case at least, two pulses of flows were involved. Also, several, smaller-scale, normally graded layers were deposited semi-continuously by several smaller flows or are the result of velocity pulsing (*sensu* Best *et al.*, 2005). Additional explanations for the changing flow are discussed below in the section on the origin of the clay-rich flows. The thicker 'atypical' beds possibly reflect several, larger pulses of flow.

A gradual, bioturbated, upward transition to the overlying bed of FA2 shows that biological activity resumed after passage of the flow(s). In the case of an abrupt upper boundary, this surface is interpreted as a slip plane above which material was removed. The slip plane was buried rapidly by flows or slumps from a head scarp, thus preventing bioturbation of the boundary. Such failures affected the stratigraphic organization of the fjord-marine deposit as presented in the following section.

STRATIGRAPHIC ORGANIZATION

The fjord-marine deposits in the bay of Trondheim consist of the four facies associations FA1 to FA4 and a schematic presentation of the overall stratigraphy is given in Fig. 4. Facies Association 2 dominates and generally is more fine-grained in the deeper part of the stratigraphy as shown in GS08. Facies Association 1 is found mostly on the sea bed and is especially thick near land (Core 1-1; Fig. 4). Facies Association 4 is found throughout the succession in the western part of the Trondheim embayment. Most beds are found in the younger part (Fig. 3). Thicker beds of FA3 are found in the eastern part of the embayment and in a few cores to the west (for example, at 1 m in Core GS08, Figs 3 and 7A).

The seismic reflection pattern shows that the main bedding in the deposits is near-horizontal or parallel to the sea bed as is typical for fjord-marine sediments (Fig. 4). However, a few clear unconformities draped by sediments are represented by truncated reflectors. Reflectors are also truncated at the sea bed inside relatively young slide scars along the Nidelva Channel (Fig. 1). A few slide scars mapped on the bathymetry in Fig. 1 are less clearly defined and are draped by sediments. These scars are pre-historic and one such scar possibly correlates with a truncation surface in the seismic profile (upper stippled red line in Fig. 4). The sharp upper boundaries of clay-rich beds at 1·5 m depth in Core 12 and at 2·3 m depth in Core GS08, with similar ^{14}C ages above, possibly correspond to this truncation surface. However, this observation cannot be verified with certainty since the cores were retrieved *ca* 100 m from the seismic line. In several cores the sharp upper boundaries of clay-rich beds are overlain by thin sand beds of FA2 and/or deformation structures are present. These beds reflect mobilized sediment that rapidly came to rest on the sliding surface.

The recognition of erosion surfaces in the stratigraphic record can also be obtained by comparing the stratigraphy of ^{14}C-dated cores (Fig. 5). Two cores were sampled from both within and outside of a diffuse, sediment-draped, slide scar north of the Nidelva Channel. The base of the scar is flat indicating that all debris was removed during mass wasting. A stratified clay-rich bed of FA4 is present in Core 9 but not in Core 4, although the lowermost ^{14}C ages in both cores are similar (Fig. 5). Instead of a clay-rich bed in the latter core, there is only a thin, greyish, fine-grained layer of FA2, interpreted as representing the sliding plane (Fig. 5); in support of this, the average sedimentation rate retrieved from the dates in Core 4 is *ca* 0·3 mm year^{-1}. This value is low compared to the average sedimentation rates for the entire deposits of 1 to 4 mm year^{-1} (L'Heureux *et al.*, 2009) and suggests that some sediment has been removed. Together, this evidence shows that failure may follow the clay-rich beds of FA4. It also indicates that some of the thin, fine-grained beds in FA2 may, in fact, represent submarine landslide failure surfaces and not small-scale depositional events. This indication clearly illustrates that detailed correlation of cores is difficult without any morphological information, seismic data or age control as available for the present study (Fig. 4). Although resedimentation processes have occurred and at least one truncation surface has been identified in Core GS08 at 2·3 m, this core is considered as covering most of the stratigraphy of the last *ca* 7500 years.

ORIGIN OF CLAY-RICH EVENT BEDS

There are several arguments in support of the notion that the clay-rich beds of FA4 accumulated during sudden events with an increased supply of fines to the fjord. The beds display relatively low TOC values, indicating that they do not originate from mass wasting of the surrounding marine sediments (FA2) with higher TOC values (for example, Fig. 3). A different origin is also supported by a slightly different mineral composition. Some samples show that the source for FA2 includes an input from the local chlorite-enriched bedrock, whereas FA4 is dominated by a source less markedly enriched in chlorite. A likely source is the emerging glaciomarine clays around Trondheim described by Reite (1983). The thicker, clay-rich event beds of FA3 and FA4 possibly represent significant sometimes composite events whereas the thinner, greyish, fine-grained beds within FA2 reflect smaller events, if not representing actual failure planes or deformations as discussed above. The stratified event beds of FA4 are considered as having been deposited relatively fast and were too thick to be destroyed by subsequent bioturbation. The bioturbated, clay-rich beds of FA3 were deposited more slowly or in smaller pulses, thus allowing bioturbation to destroy most of the sedimentary structures. Facies Association 3, which is slightly finer grained than FA4, was possibly deposited laterally or distally to FA4.

Large, terrestrial quick-clay landslides

The most likely source for the sudden increased supply of clay to the fjord is large, (pre-)historic, terrestrial, quick-clay landslides (L'Heureux *et al.*, 2009). Such landslides, also called clay-flow slides or earth flows (Mitchell & Markell, 1974; Hungr *et al.*, 2001), are well-documented in the valleys around Trondheim and are known to have occurred on several occasions during the Holocene (Fig. 1B; Reite, 1983; Sveian *et al.*, 2007; L'Heureux *et al.*, 2009). Some of these landslides involved as much as 60×10^6 m^3 of sediments (Sand, 1999). An illustration of such an event is given in Fig. 12. A common natural trigger for quick-clay landslides is river erosion (e.g. Bjerrum *et al.*, 1969, 1971; Lebuis *et al.*, 1983; Geertsema *et al.*, 2006a). However, strong earthquakes can also trigger such landslides (e.g. Updyke *et al.*, 1988). Quick-clay landslides have also been reported from along the shoreline (e.g. Longva *et al.*, 2003). Human activity can also trigger quick-clay landslides.

Large quick-clay landslides along a river can generate an initial flood wave propagating both up and downstream of the landslide crater (e.g. Schwab *et al.*, 2004). Commonly, a large portion of the debris collapses and develops into what could be called thick suspensions, viscous fluids/liquids or slurries (Bjerrum, 1955; Ter-Stepanian, 2000; Hungr *et al.*, 2001). Resistance to flow of clay suspensions is especially low on gravel beds (Wang *et al.*, 1998). Large slabs of landslide debris are often transported by these suspensions (Ter-Stepanian, 2000). Debris may block a river entirely, as is commonly observed for landslides involving sensitive clays and silts (e.g. Kenney, 1968; Løken *et al.*, 1970; Schwab *et al.*, 2004; Geertsema *et al.*, 2006b) and landslide masses

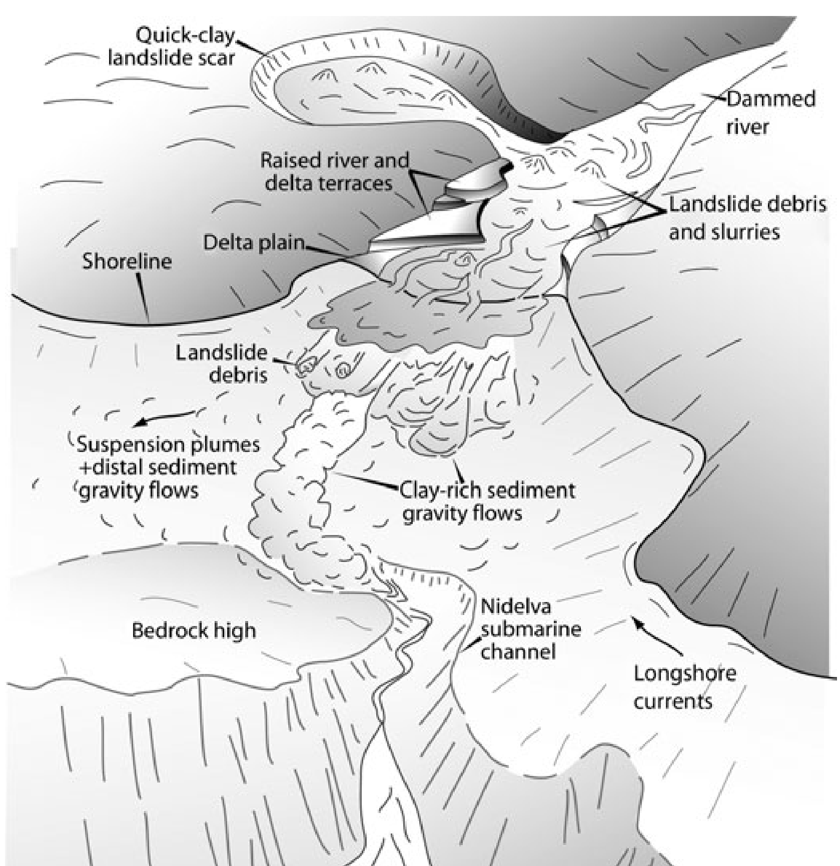

Fig. 12. Simplified palaeoenvironmental reconstruction of quick-clay landslide and transport of liquefied quick-clay and landslide debris into the fjord.

may fill a river channel for several kilometres (e.g. Løken *et al.*, 1970). Dams generated by quick-clay landslides generally have relatively low relief and subsequent erosion of the cohesive sediments therefore takes some time (Brooks *et al.*, 2001). Modern examples show that dam breaching often occurs hours to months after large landslides (e.g. Løken *et al.*, 1970; Brooks *et al.*, 2001). In several historical cases, landslide masses have been excavated by man to restore the river back to a controlled path (e.g. Løken *et al.*, 1970). The size of the dam depends on the width of the river valley, channel morphology and the size of the quick-clay landslide. With an increasing distance between the landslide and the fjord, and/or during smaller landslides, the clay-rich suspensions become progressively diluted downstream. In Trondheim, clay deposits partially filled the outlet of the Nidelva River following the Tiller landslide in 1816 (Fig. 1C) and, for this reason, a new harbour was subsequently constructed outside the river mouth (Helland, 1898). Clay-rich layers discovered through drilling on land in Trondheim are interpreted as landslide debris that accumulated in river channels and banks (e.g. Sandvik, 1995; Reite *et al.*, 1999).

Sediment transport and deposition in the fjord

If a quick-clay landslide occurs in a down-valley position or along the shore, slurries and landslide debris continue directly into the fjord. Even landslides occurring many kilometres upstream can result in deposition of thin clay beds in the fjord, as exemplified by the Tiller landslide in 1816 (supported by ^{14}C dating in Core 1-1 that contains a thin clay bed; Fig. 4). Plumes spread out as interflows, overflows or a combination of flows, depending on the character of the effluent, and flocculation will promote intense suspension settling of clay. Fast sedimentation will result in oversteepening and remobilisation. In several cases, clay-rich plumes may favour hyperpycnal flow due to their having a density in excess of that of fjord-marine water (*sensu* Mulder & Alexander, 2001; Mulder *et al.*, 2003). Seismic profiles from relatively shallow areas in the bay of Trondheim display irregular lenses interpreted as landslide debris (L'Heureux *et al.*, 2010). However, suspensions and landslide debris probably continue into deeper water in places with steeper delta fronts. Here, landslide debris and/or slurries accelerate depending on bathymetry. Landslide debris disintegrates during transport and flows are likely to become more dilute and turbulent with distance. Merging, accelerating flows in the area of the Nidelva Channel (Fig. 1D) allowed for a development into more energetic flows. Stratified flows may have occurred with a lower, mud-rich, debris flow or slurry overridden by a turbidity current (*sensu,* for example, Postma *et al.*, 1988; Lowe & Guy, 2000). Along the channel, deposition probably took place through overspill and stripping by processes summarized by Peakall *et al.* (2000).

The two-fold division of the typical beds of FA4, with a mud-rich lower part and a sandier upper part, could be explained by a reduction in the amount of clay-rich slurries and landslide debris pouring into the fjord. The re-established river flow subsequently carried less clay and relatively more sand and silt. Erosion of fluvial deposits and landslide debris could result in a temporary enhanced sediment supply and therefore a higher activity of deltaic failures. In addition, flows in the Nidelva Channel could develop over time from being stratified to being fully expanded and turbulent. Drainage of landslide dams combined with flooding during spring freshets, as suggested for other fjords (e.g. Syvitski & Schafer, 1996), is also a possible explanation for the sometimes abrupt change from the lower to the upper section of FA4. Beds of inversely graded, laminated sand and silt in the upper section (for example, Core 12; Figs 2 and 8B) reflects waxing flow and possibly hyperpycnal conditions during flooding (e.g. Mulder *et al.*, 2003). In this case, the two-fold division of the clay-rich beds is comparable to the two-fold division of event beds from the Saguenay fjord, Quebec, representing a turbiditic surge followed by dam breaching, flooding and hyperpycnal flow (St-Onge *et al.*, 2004). The thicker, stratified clay-rich beds of facies FA4 probably represent more dramatic events possibly involving several landslides or one very large and complex event.

Thicker accumulations of FA3 were deposited either gradually or episodically from flow pulses and/or suspended plumes diverted along the coast from the delta and the Nidelva Channel area. Flows are considered to have been subjected to extensive lofting and mixing with the ambient fluid and hyperpycnal flows especially may have been subjected to significant vertical flow expansion (Mulder & Alexander, 2001). Lofting led to a wide dispersal of clay particles and a reduction in the density of plumes, at the same time as mixing of salt water into the flow and erosion at its base maintained its density during further transport to the deeper fjord basin. Concentrated flows became progressively diluted with distance giving rise to a continuum of deposits (e.g. Stanley & Maldonado, 1981). Turbidite beds in the central Trondheimsfjorden may represent the distal parts of flows caused by terrestrial quick-clay landslides although the source could be outside the Trondheim area (Bøe *et al.*, 2003).

CHRONOLOGY OF MAJOR TERRESTRIAL LANDSLIDE EVENTS

Dating of mollusc shells a few centimetres below most of the clay-rich beds in Core GS08 forms the basis for a chronology of major landslide events in clays of the Trondheim bay catchment (Fig. 13). Some events could have happened along the margin of the fjord but scars have not been identified and the two-fold division of FA4 points towards a fluvial source. The events included in the present study are compared with other data sets from the central fjord basin (Bøe *et al.*, 2003) and on land (Sand, 1999; Fig. 13).

At least eight, major, landslide events have been identified (Fig. 13). The youngest event is identified in Core 1-1 with a calibrated age of *ca* 260 to 140 yr BP (Fig. 4), and probably corresponds to the Tiller landslide of 1816 (Event 1). Event 2 is represented partially by a bioturbated bed in Core GS08 at 1 m depth and dating gives a calibrated age of 1415 to 1320 yr BP (Fig 3). Another partially bioturbated bed of similar age is recorded at 1·5 m in Core 5-7 (Fig. 4). The beds accumulated distally to the outlet of the Nidelva River that had moved eastwards according to L'Heureux *et al.* (2009). Beds of Events 3, 4, 5 and 6 accumulated as the outlet of the Nidelva River was located further to the west near the head of the Nidelva Channel (Fig. 1D), and are well-stratified, 'typical' clay-rich beds. Event 3 is dated

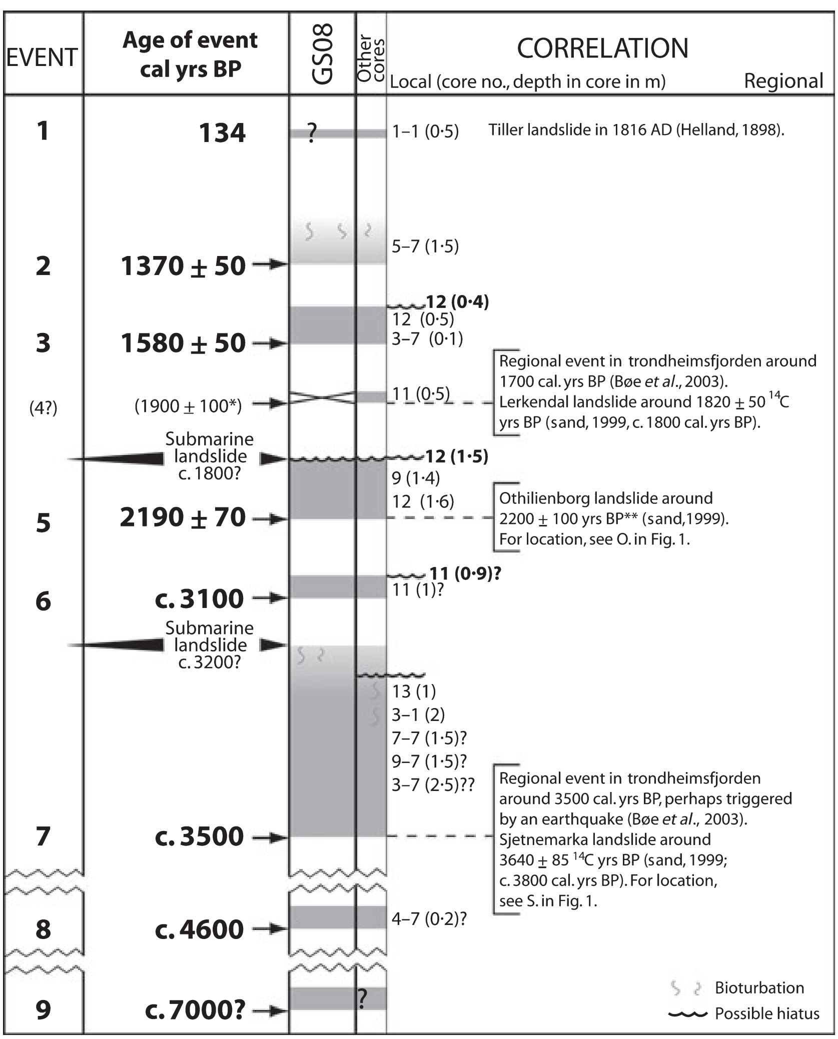

Fig. 13. Chronology of major terrestrial quick-clay landslides near Trondheim. The chronology is primarily based on dates from Core GS08. Age marked by an asterisk (*) is from L'Heureux *et al.* (2009) (TUa6338). Event 4 is represented in Core 11, which may have been affected by submarine sliding (Fig. 4) and, therefore, the event is considered as uncertain.

to 1630 to 1530 cal yr BP in Core GS08 (Fig. 3). Event 4 is not recorded in GS08 but is only represented by an indistinct bed in Core 11 and, therefore, is considered as uncertain or of little significance (Figs 4 and 13). Beds of Event 5, dated in Core GS08 to *ca* 2260 to 2115 cal yr BP (Fig. 3), are relatively thick and a sharp top is present in several cores; this indicates that a submarine landslide took place sometime after Event 5 and is possibly represented by the old, sediment-draped, slide scar west of Core GS08 (Fig. 1D). Event 6 is represented in GS08 where it is dated to a maximum of 3205 to 3070 cal yr BP (Fig. 3). The thick, 'atypical' bed of Event 7 is recognized in several cores and represents one major or several superimposed event(s). The younger age in Core 3-1 of 3690 to 3550 cal yr BP is considered as a maximum for Event 7. A similar age of 3685 to 3590 cal yr BP is given at the base of the bed(s) in Core GS08. Some dated mollusc shells within the thick bed give older, inverted ages and are reworked. It follows that deposition initiated after 3600 cal yr BP and corresponds to the 3500-year event described by L'Heureux *et al.* (2009). An age of *ca* 3200 cal yr BP is retrieved at a distance above the upper boundary of the thick bed of Event 7, showing that deposition finished well before this time. The dates support the interpretation that the thick bed was deposited relatively quickly. Only two beds are found at greater stratigraphic depths in Core GS08, representing Events 8 and 9. Event 8 occurred around a maximum of 4600 yr BP as shown by radiocarbon dating (4690 to 4530 cal yr BP; Fig. 3). An average sedimentation rate of *ca* 1·7 to 2·0 mm year^{-1} can be calculated from the two oldest dates in Core GS08. Event 9 is older than *ca* 6100 cal yr BP and the age is possibly *ca* 7000 years as calculated through extrapolation using the above sedimentation rate. In the same way, the base of Core GS08 can be calculated to being *ca* 7500 cal yr BP.

River erosion was a possible trigger for most of the terrestrial landslide events recorded at the fjord-marginal position at Trondheim, although seismic events cannot be excluded. The thick, 'atypical' bed of Event 7 could possibly be a result of one very large, complex landslide or several landslides happening within a short period of time. This effect could be the result of a relatively strong earthquake affecting the entire catchment. The occurrence of a major earthquake is supported by regional studies in Trondheimsfjorden showing that widespread mass wasting events took place at *ca* 3500 cal yr BP (Bøe *et al.*, 2003). This record includes a clay-rich turbidite in the central fjord. A major unconformity in the seismic profile (Fig. 4), near the base of GS08 could potentially be contemporary with the Storegga event *ca* 8100 cal yr BP (Haflidason *et al.*, 2005), but more dates are needed for confirmation.

Depositional trends in the Holocene sedimentary record

The overall upward coarsening tendency described for FA2 is, at least to some extent, explained by progradation and filling of the fjord during a fall of relative sea-level. Variations during this overall tendency are explained by changes in sediment supply due to lateral migration of the river outlet, changes of flow activity and of mass-wasting events on land and in the fjord. However, the detailed record of minor events in the fjord and on land is being 'compromised' by bioturbation. Ages of *ca* 1800 and 3200 cal yr BP are suggested for two major, inferred submarine landslide events (buried slide scars in Fig. 4).

The increased frequency of major, terrestrial landslides in the later part of the Holocene is explained by a combination of factors. A high relief with deep incision of rivers during a late stage of glacioisostatic uplift following the Ice Age is considered as a major factor. Also, a generally wetter and colder climate in the late Holocene (e.g. Nesje *et al.*, 2005) could have increased river erosion and long-term changes in ground water conditions favouring formation of quick clay. An implication is that the turbiditic beds in this fjord-marginal position are not linked directly to flood frequencies but primarily to the presence of unstable slopes with quick clay in the catchment resulting in sudden influxes of fines to the fjord.

It may be no coincidence that the lowermost event bed in GS08 (i.e. the most distal to sediment sources since the area has experienced a continuous relative sea-level fall; Fig. 1C) has a relatively well-developed sandy layer at the base compared to the other event beds. Such a bed is also found in the central part of Trondheimsfjorden (at *ca* 3500 cal yr BP; Bøe *et al.*, 2003). This finding possibly testifies to more well-developed, turbulent flows in distal areas facilitating improved segregation of grain sizes. It may also reflect a previously lower relief of the Nidelva Channel (L'Heureux *et al.*, 2009) allowing for more overspill from the main flow.

INHERITED WEAKNESS OF CLAY-RICH EVENT BEDS

The clay-rich beds of FA4 show lower shear strength when compared to the surrounding facies associations (Fig. 2). In addition, the above study of cores adds to the growing evidence that submarine failures can follow the event beds of FA4 and possibly also FA3 (Figs 4, 5 and 8A; see also L'Heureux *et al.*, 2010). The sedimentological properties are examined below to better understand their inherent weakness.

Mineralogy is considered to contribute to the weakness of the clay-rich beds as the finer grain sizes consist of glacially produced rock flour of inactive minerals that favour high sensitivities (loss of strength when disturbed), similar to widespread clay deposits in Scandinavia and Canada (Torrance, 1983, 1991). In addition, the studied sediment is texturally immature with angular, irregular grains and abundant, platy particles and high contents of silt. Sorting is poor and the facies varies in a continuum from grain-supported silt/fine sand with a skeletal fabric of equant grains and mica, to a matrix-dominated mud locally displaying a honeycomb fabric with grains of coarser silt in an open structure (Fig. 10). An open, flocculated particle arrangement (honeycomb fabric) is characteristic for soft, highly sensitive clay deposits (Mitchell, 1993; Selby, 2005). Changes in the electrolytical environment, for example, caused by ground water leaching may reduce the bindings between particles (Rosenquist, 1953). In this case, the texturally immature sediment with numerous silt grains in a flocculated mud matrix would possibly destabilize more easily than, for example, a sediment dominated solely by flocculated mud. The mud matrix may hinder a closer packing of coarser, equant grains and a loose packing in coarser-grained facies can also affect stability (*sensu* Mitchell, 1993). This effect is facilitated by irregular particle shapes favouring low densities and high porosities. An important weakening factor is the anisotropy of FA4 and of the deposit in general, with layers of both low and high permeability. Low-permeability barriers of mud affect ground water flow and pore-pressure response following a rapid change in boundary conditions due to, for example, erosion, high sedimentation rates, earthquakes and/or construction activity (e.g. Kokusho, 1999; Kokusho & Kojima, 2002; Malvick *et al.*, 2002). The common presence of mica flakes aligned parallel to bedding (fabric anisotropy) also reduces soil strength and facilitates the development of failure planes (e.g. Hein, 1991; Hight & Leroueil, 2003). It follows from the above that the weakness of the clay-rich beds can be attributed, in part, to the nature of their source and modes of deposition such as varying suspended concentrations and turbulence, varying degrees of grain-size segregation, pulsating flow and fast sedimentation. The clay-rich beds also have a low organic content and display little sign of biological activity which may play a role in the development of strength (Perret *et al.*, 1995). Long-term compaction and consolidation usually increase soil strength with time and depth of burial.

The detection of weak layers is of importance for the assessment of slope stability of near-shore areas, for example, in fjords (e.g. Longva *et al.*, 2003). The clay-rich event beds from the bay of Trondheim have special characteristics that seem to make them prone to failure. Weak layers similar to those presented in this study could be important for the stability of other near-shore areas. Such areas are present in similar uplifted fjord valleys with sensitive glaciomarine sediments in, for example, Canada and Scandinavia. A precondition for the accumulation of event beds as described here is the record of prehistoric landslides in clays in the catchment and a gentle to moderately sloping fjord margin on which the turbiditic beds may accumulate.

CONCLUSIONS

- The clay-rich event beds in the bay of Trondheim were deposited rapidly by turbiditic flows caused by large, terrestrial, quick-clay landslides during which debris and slurries poured into the fjord. Rapid deposition gave rise to burial of benthonic communities, which resulted in the preservation of primary sedimentary facies within the otherwise bioturbated, fjord-marine deposits.
- Stratified or bioturbated clay-rich beds are present depending on the size and position of the landslide event(s), position of the river outlet, bathymetry, the rate of deposition, and the biological activity on the sea bed. The bioturbated beds are possibly lateral or distal equivalents of the stratified beds. The latter generally were deposited as overspill along a submarine channel.
- 'Typical' stratified beds contain a lower, fine-grained section deposited initially by a muddy surge. The upper, slightly sandier, section

possibly reflects a decrease in the supply of mud following the landslide. Breaching of landslide dams, flooding and an increased activity of delta-derived sediment gravity flows can also have played a role. Subsequently, several beds seem to be composed of several turbidites following one landslide event. Exceptionally thick, stratified 'atypical' successions with a less clear organization can reflect the occurrence of several, complex landslides within a short period of time.

- A chronology based on ^{14}C dating has been established for at least eight, major, terrestrial landslide events. The record displays an increasing landslide activity during the Holocene. This activity is linked to deep fluvial incision, high relief and quick-clay development in clays following long-term glacioisostatic uplift, possibly with a climatic influence. One or more pronounced event(s) occurred at *ca* 3500 cal yr BP, possibly triggered by an earthquake.
- The event beds are texturally immature and are characterized by angular grains, inactive minerals, abundant mica and poor sorting. Composition varies from grain-supported, with or without a matrix of mud with honeycomb fabric, to mud with varying amounts of coarser silt grains.
- Several hiati from submarine failures have been identified. Failure planes follow the clay-rich beds which represent weak layers in the fjord-marine record; their inherent weakness is related, in part, to their origin and modes of deposition affecting their composition, texture, structure and permeability.
- Preconditions for the accumulation of clay-rich, slide-prone beds are the presence of quick clay in the hinterland and a moderately sloping fjord margin. The presence of similar landslide-derived turbiditic beds possibly plays an important role for the stability of near-shore slopes in other glacioisostatically uplifted fjord valleys.

ACKNOWLEDGEMENTS

This work was carried out with financial support from NGU and the International Centre for Geohazards (ICG) within a project on 'Offshore geohazards'. The work was also supported by the Norwegian Road Authority and the Trondheim Harbour Authority. We thank Haflidi Haflidason for giving us access to the logging and sedimentological laboratories of the Department of Earth Science, University of Bergen. We acknowledge the *R/V Seisma*, *R/V Gunnerius* and *R/V GO Sars* crew members and participants for invaluable assistance during data acquisition. We thank Adrian Palmer, Department of Geography, Royal Holloway, University of London, for preparation of thin sections. Øyvind Stokland helped with the identification of mollusc shells. We thank Gjermund Vingerhagen for his assistance during project work and Shana Volesky for counting mineral grains. Bjørn Willemoes-Wissing helped with SEM. We thank Vegar Johansen (SINTEF) for permission to publish data from Core GS08 collected during the SOSS project. Associate Editor Jess Trofimovs and two anonymous reviewers gave constructive comments on the manuscript. It also benefited from comments by Miquel Canals and Anders Solheim. We are grateful to David Roberts for correcting the English language. This is Contribution No. 303 from the International Centre for Geohazards (ICG), Norway.

REFERENCES

Baas, J.H. and **Best, J.L.** (2002) Turbulence modulation in clay-rich sediment-laden flows and some implications for sediment deposition. *J. Sed. Res.*, **72,** 3.

Baas, J.H. and **Best, J.L.** (2008) The dynamics of turbulent, transitional and laminar clay-laden flow over a fixed current ripple. *Sedimentology*, **55,** 635–666.

Bennett, R.H., Bryant, W.R. and **Keller, G.H.** (1981) Clay fabric of selected submarine sediments: fundamental properties and models. *J. Sed. Petrol.*, **51,** 1.

Best, J.L., Kostaschuk, R.A., Peakall, J., Villard, P.V. and **Franklin, M.** (2005) Whole flow field dynamics and velocity pulsing within natural sediment-laden underflows. *Geology*, **33,** 765–768.

Bjerrum, L. (1955) Stability of natural slopes in quick clay. *Geotechnique*, **5,** 101–119.

Bjerrum, L., Løken, T., Heiberg, S. and **Foster, R.** (1969) A field study of factors responsible for quick clay slides. *Proceedings of the 7th International Conference on Soil Mechanics and Foundation Engineering*, Mexico, Vol. 2, pp. 531–540.

Bjerrum, L., Løken, T. and **Heiberg, S.** (1971) A field study of factors responsible for quick clay slides. *Norw. Geotech. Inst. Publ.*, **85,** 17–36.

Bøe, R., Rise, L., Blikra, L.H., Longva, O. and **Eide, A.** (2003) Holocene mass-movement processes in Trondheimsfjorden, Central Norway. *Norw. J. Geol.*, **83,** 3–22.

Bouma, A.H. (1962) *Sedimentology of Some Flysch Deposits: A Graphic Approach to Facies Interpretation*. Elsevier, Amsterdam, 168 pp.

Bronk Ramsey, C. (2001) Development of the Radiocarbon Program Oxcal. *Radiocarbon*, **43**(2A), 355–363.

Brooks, G.R., Evans, S.G. and **Claque, J.J.** (2001) Floods. In: *A Synthesis of Geological Hazards in Canada* (Ed. G.R. Brooks), *Geol. Surv. Can. Bull.*, **548,** 101–143.

Cramp, A., Lee, S.V., Herniman, J., Hiscott, R.N., Manley, P.L., Piper, D.J.W., Deptuck, M., Johnston, S.K. and **Black, K.S.** (1997) Interlaboratory comparison of sediment grain-sizing techniques: data from Amazon Fan Upper Levee

Complex Sediments. In: *Proceedings of the Ocean Drilling Program, Scientific Results, 155*. (Eds R.D. Flood, D.J.W. Piper, A. Klaus and L.C. Peterson), pp. 217–228. Ocean Drilling Program, College Station, TX.

Einsele, G., Chough, S.K. and **Shiki, T.** (1996) Depositional events and their records – an introduction. *Sed. Geol.*, **104,** 1–9.

Flemming, B.W. (2000) A revised textural classification of gravel-free muddy sediments on the basis of ternary diagrams. *Cont. Shelf Res.*, **20,** 1125–1137.

Friedman, G.M. and **Sanders, J.E.** (1978) *Principles of Sedimentology*. John Wiley and Sons, New York, 792 pp.

Geertsema, M., Claque, J.J., Schwab, J.W. and **Evans, S.G.** (2006a) An overview of recent large catastrophic landslides in Northern British Columbia, Canada. *Eng. Geol.*, **83,** 120–143.

Geertsema, M., Cruden, D.M. and **Schwab, J.W.** (2006b) A large rapid landslide in sensitive glaciomarine sediments at Mink Creek, northwestern British Columbia, Canada. *Eng. Geol.*, **83,** 36–63.

Haflidason, H., Lien, R., Sejrup, H.P., Forsberg, C.F. and **Bryn, P.** (2005) The dating and morphometry of the Storegga Slide. *Mar. Petrol. Geol.*, **22,** 123–136.

Hansen, L., Eilertsen, R. and **Longva, O.** (2005) *Skredkartlegging langs kystsonen i Trondheimsområdet, datagrunnlag og morfologi*. Geological Survey of Norway Report 2005.054, Trondheim, 27 pp. [In Norwegian]

Hansen, L., Eilertsen, R., Solberg, I.L., Sveian, H. and **Rokoengen, K.** (2007) Facies characteristics, morphology and depositional models of clay-slide deposits in terraced fjord valleys, Norway. *Sed. Geol.*, **202,** 710–729.

Hein, F.J. (1991) The need for grain size analyses in marine geotechnical studies. In: *Principles, Methods and Application of Particle Size Analysis* (Ed. J.P.M. Syvitski), pp. 346–362. Cambridge University Press, New York.

Helland, A. (1898) *Topografisk-statistisk beskrivelse av Søndre Trondheims Amt. Første del: Den almindelige del og Trondhjem*. Norges Land og Folk XVI. Olaf Norlis, Kristiania [In Norwegian]

Hight, D.W. and **Leroueil, S.** (2003) Characterisation of soils for engineering purposes. In: *Characterisation and Engineering properties of Natural Soils* (Eds T.S. Tan, K.K. Phoon, D.W. Hight and S. Leroueil), pp. 255–362. Swetz & Zeitlinger, Lisse, The Nederlands.

Hughen, K.A., Baillie, M.G.L., Bard, E., Bayliss, A., Beck, J.W., Bertrand, C., Blackwell, P.G., Buck, C.E., Burr, G., Cutler, K.B., Damon, P.E., Edwards, R.L., Fairbanks, R.G., Friedrich, M., Guilderson, T.P., Kromer, B., McCormac, F.G., Manning, S., Bronk Ramsey, C., Reimer, P.J., Reimer, R.W., Remmele, S., Southon, J.R., Stuiver, M., Talamo, S., Taylor, F.W., van der Plicht, J. and **Weyhenmeyer, C.E.** (2004) Marine04 marine radiocarbon age calibration, 0-26 Cal Kyr BP. *Radiocarbon*, **46,** 1059–1086.

Hungr, O., Evans, S.G., Bovis, M.J. and **Hutchinson, J.N.** (2001) A review of the classification of landslides of the flow type. *Environ. Eng. Geosci.*, **7,** 221–238.

Karlsrud, K., Aas, G. and **Gregersen, O.** (1985) Can we predict landslide hazards in soft sensitive clays? Summary of norwegian practice and experiences. *Norw. Geotech. Inst. Publ.*, **158,** 1–24.

Kenney, T.C. (1968) Slide behaviour and shear resistance of a quick clay determined from a study of the landslide at Selnes, Norway. *Norw. Geotech. Inst. Publ.*, **76,** 57–63.

Kokusho, T. (1999) Water film in liquefied sand and its effect on lateral spread. *J. Geotech. Geo-environ. Eng.*, **125,** 817–826.

Kokusho, T. and **Kojima, T.** (2002) Mechanism for postliquefaction water film generation in layered sand. *J. Geotech. Geo-environ. Eng.*, **128,** 129–137.

Kranck, K. (1984) Grain-size characteristics of turbidites. In: *Fine-Grained Sediments: Deep-Water Processes and Facies* (Eds D.A.V. Stow and D.J.W. Piper), pp. 83–92. Geological Society Special Publication, London.

La Rochelle, P., Chagnon, J.Y. and **Lefebvre, G.** (1970) Regional geology and landslides in the marine clay deposits of eastern Canada. *Can. Geotech. J.*, **7,** 145–156.

Lebuis, J., Robert, J.M. and **Rissman, P.** (1983) *Regional Mapping of Landslide Hazard in Quebec. Symposium on Slopes on Soft Clays*. Swedish Geotechnical Institute, Linköping, Report 17, pp. 205–262.

Lefebvre, G. (1996) Soft sensitive clays. In: *Landslides, Investigation and Mitigation*. (Eds A.K. Turner and R.L. Schuster), Special Report 247, pp. 607–619. National Academy Press, Washington D.C.

L'Heureux, J.S., Hansen, L. and **Longva, O.** (2009) Development of the Nidelv Submarine Channel in Trondheimsfjorden, Norway: implications for present slope stability. *Mar. Geol.*, **260,** 30–40.

L'Heureux, J.S., Hansen, L., Longva, O., Emdal, A. and **Grande, L.O.** (2010) A multidisciplinary study of submarine landslides at the Nidelva fjord delta, Central Norway – implications for geohazards assessment. *Norw. J. Geol.*, **90,** 1–20.

Løken, T., Jørstad, F. and **Heiberg, S.** (1970) Gamle leirskred på Romerike. *Særtrykk av Romerike Historielags årbok*, **VII,** 19.

Longva, O., Janbu, N., Blikra, L.H. and **Boe, R.** (2003) The 1996 Finneidfjord slide: seafloor failure and slide dynamics. In: *Submarine Mass Movements and Their Consequences* (Eds J. Locat and J. Mienert), pp. 531–538. Kluwer academic Publishers, Dordrecht, The Netherlands.

Lowe, D.R. and **Guy, M.** (2000) Slurry-flow deposits in the Britannia Formation, North Sea. *Sedimentology*, **47,** 31–70.

Malvick, E.J., Kulasingam, R., Kutter, B.L. and **Boulanger, R.W.** (2002) Void redistribution and localized shear strains in slopes during liquefaction. *Proceedings of the International Conference on Physical Modelling in Geotechnics*, ICPMG '02, St John's, NF, Canada, pp. 495–500.

Mangerud, J., Bondevik, S., Gulliksen, S., Hufthammer, A.K. and **Høisæter, T.** (2006) Marine ^{14}C reservoir ages for 19th century whales and molluscs from the North Atlantic. *Quatern. Sci. Rev.*, **25,** 3228–3245.

Middleton, G.V. and **Hampton, M.A.** (1973) Sediment gravity flows: mechanisms of flow and deposition. In: *Turbidites and Deep Water Sedimentation* (Eds G.V. Middleton and A.H. Bouma), pp. 1–38. Society of Economic Paleontologists and Mineralogists Pacific section, Los Angeles.

Mitchell, J.K. (1993) *Fundamentals of Soil Behavior*. John Wiley & Sons, Inc., New York, 437 pp.

Mitchell, R.J. and **Markell, A.R.** (1974) Flowsliding in sensitive soils. *Can. Geotech. J.*, **11,** 11–31.

Mulder, T. and **Alexander, J.** (2001) The physical character of subaqueous sediment density flows and their deposits. *Sedimentology*, **48,** 269–299.

Mulder, T., Migeon, S., Savoye, B. and **Jouanneau, J.-M.** (2001) Twentieth century floods recorded in the deep Mediterranean sediments. *Geology*, **29,** 1011–1014.

Mulder, T., Syvitski, J.P.M., Migeon, S., Faugères, J.-C. and **Savoye, B.** (2003) Marine hyperpycnal flows: initiation, behaviour and related deposits. A review. *Mar. Petrol. Geol.*, **20,** 861–882.

Nesje, A., Jansen, E., Birks, H.J.B., Bjune, A.E., Bakke, J., Andersson, C., Dahl, S.O., Kristensen, D.K., Lauritzen, S.-E., Lie, Ø., Risebrobakken, B. and **Svendsen, J.-I.** (2005) Holocene Climate Variability in the Northern North Atlantic Region: a Review of Terrestrial and Marine Evidence. In: *The Nordic Seas: An Integrated Perspective* (Eds H. Drange, T. Dokken, T. Furevik, R. Gerdes and W. Berger), American Geophysical Union, *Geophys. Monogr. Ser.*, **158,** 289–322.

Peakall, J., McCaffrey, B. and **Kneller, B.** (2000) A model for the evolution, morphology, and architecture of sinuous submarine channels. *J. Sed. Res.*, **70,** 434–448.

Perret, D., Locat, J. and **Leroueil, S.** (1995) Strength development with burial in fine-grained sediments from the Saguenay Fjord, Quebec. *Can. Geotech. J.*, **32,** 247–262.

Postma, G., Nemec, W. and **Kleinspehn, K.L.** (1988) Large floating clasts in turbidites: a mechanism for their emplacement. *Sed. Geol.*, **58,** 47–61.

Reite, A.J. (1983) Trondheim. Desciption of the Quaternary geological map 1621 IV (scale 1 : 50.000). *Geol. Surv. Norway, Skrifter*, **391,** 1–44.

Reite, A.J., Sveian, H. and **Erichsen, E.** (1999) Trondheim fra istid til nåtid –landskapshistorie og løsmasser. *Gråsteinen*, **5,** 40, Geological Survey of Norway. [In Norwegian]

Rosenquist, I.T. (1953) Considerations on the sensitivity of Norwegian quick-clays. *Géotechnique*, **3,** 195–200.

Rosenqvist, I.T. (1966) Norwegian research into the properties of quick clay – a review. *Eng. Geol.*, **1,** 445–450.

Sand, K. (1999) Fra istid til Nidarnes. Unpublished Report, 116 pp. [In Norwegian]

Sandvik, P.U. (1995) The archbishops Palace, Trondheim. Results from the archeobotanical investigations in 1991. *Res. Archaeobotanicae – 9th Symposium IWGP*, Kiel, pp. 267–279.

Scheiber, J., Southard, J. and **Thaisen, K.** (2007) Accretion of mudstone beds from migrating floccule ripples. *Science*, **318,** 1760–1762.

Schnellmann, M., Anselmetti, F.S., Giardini, D. and **McKenzie, J.A.** (2006) 15,000 Years of mass-movement history in Lake Lucern: implications for seismic and tsunami hazards. *Eclogae Geol. Helv.*, **99,** 409–428.

Schwab, J.W., Geetsema, M. and **Blais-Stevens, A.** (2004) The Khyex River landslide of November 28, 2003, Prince Rupert British Columbia, Canada. *Landslides*, **1,** 243–246.

Selby, M.J. (2005) *Hillslope Materials and Processes*, 2nd edn. Oxford University press, Oxford, 451 pp.

Selmer-Olsen, R. (1977) *Ingeniør geologi del 2, de løse jordlag.* Tapir, Norway, 289 pp. [In Norwegian]

Sergeyev, Y.M., Grabowska-Olszewska, B., Osipov, V.I., Sokolov, V.N. and **Kolomenski, Y.N.** (1980) The classification of microstructures of clay soils. *J. Microsc.*, **120,** 237–260.

Solli, A., Grenne, T., Slagstad, T. and **Roberts, D.** (2003) *Bedrock Map Trondheim 1621 IV, M 1 : 50 000.* Geological Survey of Norway, Trondheim.

Stanley, D.J. and **Maldonado, A.** (1981) Depositional models for fine-grained sediment in western Hellenic Trench, Eastern Mediterranean. *Sedimentology*, **28,** 273–290.

St-Onge, G., Mulder, T., Piper, D.J.W., Hillaire-Marcel, C. and **Stoner, J.S.** (2004) Earthquake and flood-induced turbidites in the Saguenay Fjord (Québec): a Holocene paleoseismicity record. *Quartern. Sci. Rev.*, **23,** 283–294.

Stow, D.A.V. and **Bowen, A.J.** (1980) A physical model for the transport and sorting of fine-grained sediments by turbidity currents. *Sedimentology*, **27,** 31–46.

Stow, D.A.V. and **Piper, D.J.W.** (1984) Deepwater fine-grained sediments: facies models. In: *Fine-Grained Sediments: Deep-Water Processes and Facies* (Eds D.A.V. Stow and D.J.W. Piper), pp. 611–646. Geological Society Special Publication, London.

Stuiver, M. and **Reimer, P.J.** (1987) A computer program for radiocarbon age calibration. *Radiocarbon*, **28,** 1022–1030.

Sveian, H., Dahl, R. and **Løvø, G.** (2007) Nidelva fra istid til Brattøra. In: *Nidelva, Trondheims hjerte* (Eds E. Fremstad and P.G. Thingstad), pp. 14–31. NTNU, Vitenskapsmuseet, Trondheim, Norway. Bli med ut! **7**. [In Norwegian]

Syvitski, J.P.M. and **Schafer, C.T.** (1996) Evidence for an earthquake-triggered basin collapse in Sagueney Fjord, Canada. *Sed. Geol.*, **104,** 127–153.

Syvitski, J.P.M., LeBlanc, K.W.G. and **Asprey, K.W.** (1991) Interlaboratory interinstrumentation calibration experiment. In: *Principles, Methods and Application of Particle Size Analysis* (Ed. J.P.M. Syvitski), pp. 174–193. Cambridge University Press, New York.

Ter-Stepanian, G. (2000) Quick clay landslides: their enigmatic features and mechanism. *Bull. Eng. Geol. Environ.*, **59,** 47–57.

Torrance, J.K. (1983) Towards a general model of quick clay development. *Sedimentology*, **30,** 547–555.

Torrance, J.K. (1991) Influences on the rheology of marine sediments composed of low-activity minerals. In: *Frontiers in Sedimentary Geology: Microstructure of Fine-Grained Sediments* (Eds R.H. Bennett, W.R. Bryant and M.H. Hulbert), pp. 509–514. Springer, New York.

Updyke, R.G., Egan, J.A., Moriwaki, Y., Idriss, I.M. and **Moses, T.L.** (1988) A model for earthquake-induced translator landslides in Quaternary sediments. *Geol. Soc. Am. Bull.*, **100,** 783–792.

Wang, Z.Y., Larsen, P., Nestman, F. and **Dittrich, A.** (1998) Resistance and drag reduction of flows of clay suspensions. *J. Hydraul. Eng.*, **124,** 41–49.

Manuscript received 20 April 2009; revision accepted 14 July 2010